PDE8 controls CD4$^+$ T cell motility through the PDE8A-Raf-1 kinase signaling complex

Chaitali P. Basole[1], Rebecca K. Nguyen[1], Katie Lamothe[1], Amanda Vang[1,2], Robert Clark[1], George S. Baillie[3], Paul M. Epstein[4], and Stefan Brocke[1]*

[1]Department of Immunology, UConn Health, [2]The National Hospital of Faroe Islands, [3]Institute of Cardiovascular and Medical Sciences, University of Glasgow, [4]Department of Cell Biology, UConn Health

*Corresponding author: sbrocke@uchc.edu

Abstract

The levels of cAMP are regulated by phosphodiesterase enzymes (PDEs), which are targets for the treatment of inflammatory disorders. We have previously shown that PDE8 regulates T cell motility. Here, for the first time, we report that PDE8A exerts part of its control of T cell function through the V-raf-1 murine leukemia viral oncogene homolog 1 (Raf-1) kinase signaling pathway. To examine T cell motility under physiologic conditions, we analyzed T cell interactions with endothelial cells and ligands in flow assays. The highly PDE8-selective enzymatic inhibitor PF-04957325 suppresses adhesion of *in vivo* myelin oligodendrocyte glycoprotein (MOG) activated inflammatory CD4$^+$ T effector (Teff) cells to brain endothelial cells under shear stress. Recently, PDE8A was shown to associate with Raf-1 creating a compartment of low cAMP levels around Raf-1 thereby protecting it from protein kinase A (PKA) mediated inhibitory phosphorylation. To test the function of this complex in Teff cells, we used a cell permeable peptide that selectively disrupts the PDE8A-Raf-1 interaction. The disruptor peptide inhibits the Teff–endothelial cell interaction more potently than the enzymatic inhibitor. Furthermore, the LFA-1/ICAM-1 interaction was identified as a target of disruptor peptide mediated reduction of adhesion, spreading and locomotion of Teff cells under flow. Mechanistically, we observed that disruption of the PDE8A-Raf-1 complex profoundly alters Raf-1 signaling in Teff cells. Collectively, our studies demonstrate that PDE8A inhibition by enzymatic inhibitors or PDE8A-Raf-1 kinase complex disruptors decreases Teff cell adhesion and migration under flow, and represents a novel approach to target T cells in inflammation.

Keywords:
PDE8
CD4$^+$ T cells
Integrins
Autoimmunity
T cell motility,
Inflammation

1. Introduction

Ligand binding to Gs-coupled receptors leads to the generation of the second messenger cAMP following activation of the enzyme adenylyl cyclase. Stimulation of the T cell antigen receptor (TCR) also leads to elevation of cAMP which is known to inhibit T cell proximal signaling, IL-2 production and T cell proliferation [1, 2]. cAMP exerts these inhibitory effects in T cells through cAMP dependent protein kinase (PKA) which blocks the mitogen-activated protein kinase (MAPK) and nuclear factor of activated T cells (NFAT) dependent signaling pathways [3]. The inhibitory action of cAMP is eliminated through the action of phosphodiesterase (PDE) enzymes that hydrolyze cAMP. PDEs 3B, 4A, 4B, 4D, 7A1, 7A3 and 8A1 are the isoforms expressed in T cells [4-8]. V-raf-1 murine leukemia viral oncogene homolog 1 (Raf-1) is an upstream regulator of the MAPK-extracellular signal–regulated kinase **(**ERK)1/2 module, which controls many fundamental biological processes, including T cell proliferation, survival and adhesion [9-12]. In this pathway Raf-1 phosphorylates and activates MAP/ERK kinase (MEK)1/2, which in turn phosphorylate and activate ERK1/2. ERK has more than 150 known substrates [9, 12], which mediate many of the pleiotropic functions of this pathway [13, 14]. Raf-1 regulation is complex and is still insufficiently understood. Critical events are the dephosphorylation of an inhibitory site, S259, which allows Raf-1 binding to activated rat sarcoma viral oncogene (Ras) and is a prerequisite for further activation. S259 is a target for phosphorylation by PKA [15-17], a family of enzymes whose activity is dependent on local intracellular levels of cAMP. Thus, S259 is a primary target of a complex system of crosstalk between the cAMP and the Raf-1-ERK signaling pathways. A recent report demonstrated that Raf-1 kinase binds to PDE8A in a signaling complex, which acts to protect Raf-1 from inhibitory phosphorylation by PKA [18-20]. Our previous work has shown that PDE8 controls T cell and breast cancer cell motility [6, 21-23]. Our goal here was to delineate the mechanism by which PDE8 controls distinct categories of T cell motility and determine its selective effect on regulatory and effector components of the T cell immune response.

Our recent work shows that $CD4^+$ T cells isolated from the hilar lymph nodes draining lung tissue have increased PDE8A expression during the acute inflammatory stage in an ovalbumin induced allergic airway disease mouse model [24]. This further supports the concept of targeting PDE8A in inflammation. Recently, there has been a surge of interest in the cAMP specific PDE8 family of enzymes. PDE8 is expressed widely in human tissue [25] with functions in testosterone production [26], lymphocyte adhesion and chemotaxis [6, 21-23]. T cell activation induces cAMP and PDEs, including PDE8A, a cAMP-specific PDE with 40-100-fold greater affinity for cAMP than PDE4 [2, 5, 22, 27]. This unique feature has led to the suggestion that PDE8 enzymes may have an important role in protecting any associated protein from being affected by fluctuations in basal cAMP concentrations [5]. Compartmentalization of PDE8A in the cell to Raf-1 can regulate Raf-1 phosphorylation on S259, and, in so doing, regulate the cross-talk node whereby cAMP exerts an inhibitory effect on Raf-1 signaling [18-20], potentially affecting T cell activation and function.

Based on these observations, we hypothesized that PDE8A exerts its regulation of T cell function through the PDE8A-Raf-1 signaling pathway. Little is known regarding the specific functions of PDE8A within the immune system, especially whether the control of T cell motility is mediated through different effectors of the canonical Raf-1-ERK signaling cascade. B-Raf has been demonstrated to regulate VLA-4 integrin mediated adhesion in human T cells under shear stress independently of ERK signaling [28]. Here, we probed the PDE8A-Raf-1 kinase signaling pathway in Teff and regulatory T (Treg) cells, using specific pharmacological tools including a PDE8 inhibitor and peptide disruptor of the PDE8A-Raf-1 complex in adhesion assays under flow to assess the molecular regulation of downstream effectors of the PDE8A-Raf-1 complex.

2. Materials and Methods

2.1 Animals

Female 6-8 weeks old C57BL/6 mice were obtained from Jackson laboratories, Bar Harbor, ME. *Foxp3gfp.KI* knock-in (*Foxp3gfp*.KI) mice were obtained as a gift from Dr. Kuchroo [29]. Experiments were performed according to approved protocols at UConn Health (IACUC Protocol number 100794-1216).

2.2 Chemicals and antibodies

Recombinant mouse VCAM-1/CD106 Fc chimera (643-VM), recombinant mouse ICAM-1/CD54 Fc chimera (796-IC) were purchased from R&D systems, Minneapolis, MN. Protein A was purchased from Sigma-Aldrich (P7837). The primary antibodies for phospho-p44/42 MAPK (Thr202/Tyr204) (9101; 1:1000), p44/42 MAPK (9102; 1:1000), Phospho-Raf-1 (pSer259) (9421; 1:1000) and Raf-1 (9422; 1:1000) were purchased from Cell Signaling Technology. An additional Raf-1 antibody was purchased from BD Biosciences (610152; 1:2000). Anti-GAPDH (ab75834; 1:100,000) and anti-PDE8A antibodies (1:1000) were purchased from Abcam and Scottish Biomedical, respectively. The anti-CD3 antibody was purchased from Biolegend (100331). The secondary antibodies goat anti-rabbit IgG-HRP (65-6120, 1:4000), chicken anti-rabbit IgG-HRP (sc-2963, 1:5000) and goat anti-mouse IgG-HRP (sc-2005, 1:5000) were purchased from Invitrogen and Santa Cruz Biotechnology. The PDE8A-Raf-1 disruptor peptide (PDE8A: R454–T465; RRLSGNEYVLST) and scrambled control peptide (SYTVRLLGERNS) were synthesized as described [19]. The PDE8 selective inhibitor PF-04957325 was synthesized by Pfizer Inc., Groton, CT [6].

2.3 Isolation of Teff cells, Treg cells and $CD4^+$ T cells

$CD4^+CD25^-$ Teff and $CD4^+CD25^+$ Treg cells were isolated from the spleens of C57BL/6 mice using the $CD4^+CD25^+$ Treg Isolation kit (130-091-041, Miltenyi Biotec) as published previously [23]. For the generation of activated pathogenic $CD4^+$ T cells, C56BL/6 or *Foxp3gfp.KI* mice were immunized with myelin oligodendrocyte glycoprotein peptide 35-55 (MOG_{35-55}) in 200 µg Complete Freund's Adjuvant (CFA) (MOG_{35-55}/CFA) s.c. in the footpads [30, 31]. On d 10

post-immunization, $CD4^+$ T cells were isolated from the draining popliteal lymph nodes (PLNs) using the $CD4^+$ T cell Isolation Kit (130-104-454, Miltenyi Biotec).

2.4 Cell culture and treatments

Murine brain endothelium derived cell line bEnd.3 (ATCC, Manassas, VA) was cultured in DMEM supplemented with 100 U/ml penicillin, 100 mg/ml streptomycin, 2mM L-glutamine and 10% fetal bovine serum as described [6]. In the flow assays, endothelial cells and $CD4^+$ T cells were treated with 1 μM of the PDE8 inhibitor PF-04957325 or the DMSO vehicle control for 1 h, or with 10 μM PDE8-Raf-1 disruptor peptide or control peptide for 4 h. For the flow assay with naive Teff cells or Treg cells, cells were cultured with plate-bound anti-CD3 (10 μg/ml) with or without IL-2 (NIH) (100 Units/ml) for 18 h. For integrin expression analysis, splenic $CD4^+$ T cells isolated from *Foxp3gfp.KI* mice were cultured with plate-bound anti-CD3 (10 μg/ml) for 18 h followed by treatment with PF-04957325 or vehicle control for 1 h or disruptor or control peptide for 4 h. The cells were then pre-incubated with anti-CD16/32 (clone: 2.4 G2, 553142, BD Biosciences) for blocking Fcγ III/II receptors followed by surface staining with anti-CD4 eFluor 450 (clone: RM4-5, 48-0042, eBioscience), anti-CD11a BV510 (clone: M17/4, 563669, BD Horizon), anti-CD49d PerCp-eFluor710 (Clone: R1-2, 46-0492, eBioscience), anti-CD44 PE (clone:IM7, 553134, BD Pharmingen) antibodies. Events were acquired on LSR II (BD Biosciences). Flow cytometry data were processed on FlowJo software (Tree Star). For the Western blot experiments, $CD4^+$ T cells were treated with 1 μM PF-04957325 or 10 μM disruptor peptide and respective vehicle or scrambled peptide controls for 1or 4 h followed by plate-bound 15 min activation with 5 μg/ml plate-bound anti-CD3.

2.5 Shear stress (flow) assay

The bEnd.3 cells were stimulated with 1.25 μg/ml LPS (Sigma-Aldrich) for 18 h on d 4 after seeding. The parallel plate flow chamber (Glycotech) was assembled onto the endothelial cell plate and mounted onto the stage of an inverted phase contrast microscope (Nikon Eclipse Ti) [32]. The $CD4^+$ T cells were treated as described above and then were washed with cation free HBSS and resuspended in binding buffer [HBSS with $CaCl_2$ and $MgCl_2$, 10 mM HEPES (Life Technologies) and 2 mg/ml BSA fraction V (Roche)] at a concentration of 10^6 cells/50 μl binding buffer. The $CD4^+$ T cells were then infused over the endothelial cell layer at a constant shear flow rate using a programmable syringe pump (Harvard Apparatus). Once the cells accumulate on the bEnd.3 cells, the shear rate was increased to 5 dyn/cm^2 for the entire 15 min of the assay (migration phase) and a time-lapse video recording was done under phase contrast and GFP illumination settings using Nikon NIS imaging software. The cells and the binding buffer (entire system) were maintained at 37 °C throughout the assay. Motion analysis was done manually on all the T cells that were present in the microscopic field of view. Each T cell was individually tracked starting from the accumulation phase throughout the migration phase. Only the T cells that were present during the accumulation phase were analyzed. The distinct cell tethers that were examined are defined as follow: cells that detach

immediately after application of shear flow were considered to be detached; cells that roll on the endothelial cell surface were rolling; cells that firmly adhere to the endothelial cell surface and remain stationary for at least 1 min were defined as adhesion; cells that form non-stationary adhesion, spread and migrate along the endothelial cell surface were included in the adhesion and locomotion category, while cells that undergo transendothelial migration (TEM) were included in the adhesion and TEM category. The number of cells in each category were counted and expressed as percentage of initially accumulated cells during the accumulation phase. For flow assays with immobilized vascular ligands, recombinant VCAM-1 Fc (2 µg/ml) or ICAM-1 Fc (5 µg/ml) (in 20 mg /ml BSA in PBS) was overlaid on protein A pre-coated polystyrene plates overnight at 4 °C. Plates were then washed with PBS three times followed by blocking with 20 mg/ml BSA solution for 2 h at 37 °C. The immobilized vascular ligand coated plates were assembled as the lower wall of the flow chamber as mentioned above. The interactions of the $CD4^+$ T cells with the adhesive substrates were manually tracked as mentioned above. The cell tethers examined were rolling, transient tether, firm tether, spreading, locomotion and detachment [33]. Transient tether was defined as cells that stay for less than 4 s after flow starts, firm tether was defined as cells that stay for more than 4 s after flow starts, rolling was defined as cells that persistently rolled for at least 2 s after the flow starts, adherent cells were defined as cells that stay throughout the 15 min shear flow period. Spreading cells were defined as cells that increase their area, perimeter and also undergo darkening of the edges [34]. Cells undergoing spreading and migration were included in the locomotion category.

2.6 Western blot:

$CD4^+$ T cells were centrifuged at 2000 rpm for 5 min, washed twice with ice-cold PBS and lysed using RIPA buffer (Teknova) supplemented with protease inhibitor cocktail (1:100; Sigma-Aldrich) and phosphatase inhibitor cocktail (1:10; Roche). The lysates were then centrifuged at 10,000 rpm for 10 min to remove the cells debris. Protein concentration was determined using BCA Protein Assay kit (Pierce). Equal amounts of protein were loaded and run on 10% SDS-PAGE gel. Proteins were then transferred onto a nitrocellulose membrane (Bio-Rad Laboratories). The membrane was blocked for 1 h at room temperature with 5% non-fat dry milk in Tris- buffered saline (Bio-Rad) supplemented with 0.1% tween-20 (Sigma-Aldrich; TBS-T) before adding the primary antibodies in 5% BSA in TBS-T and incubated overnight at 4 °C. Membranes were washed three times with TBS-T, followed by incubation with horseradish-peroxidase-conjugated secondary antibody (HRP) in 5% non-fat dry milk in TBS-T at room temperature for 2 h and washed 3 more times. Proteins were visualized and quantitated with SuperSignal West Femto Maximum Sensitivity Substrate (Pierce) using Syngene G:Box with GeneSnap BioImaging software. Probing with ERK1/2 and Raf-1 antibody was used to normalize phospho ERK1/2 and phospho Raf-1 expression.

2.7 Statistical analyses:

Experimental groups were compared by analyzing data with Student's unpaired t-test using GraphPad Prism version 7.00 for Mac. Probability levels for statistically significant differences are indicated by the p value in the results and corresponding asterisks in the figures. (*P<0.05, **p<0.01, ***p<0.001, ****p≤0.0001).

3. Results

3.1 Differential motility of naive and activated Teff and Treg cells under flow.

Since PDEs and cAMP levels significantly differ between Teff and Treg cells [23, 35], we first tested $CD4^+CD25^-$ Teff and $CD4^+CD25^+$ Treg cells under naive and activating conditions for their ability to interact with LPS-activated endothelial cells (ECs) under shear flow. Mouse brain ECs were cultured as a monolayer, stimulated with LPS overnight, and the subsequent adhesive interactions with ECs were measured in the flow chamber assay. Compared to naive Teff cells, naive Treg adhered over two times more potently (11.1 ± 3.1% vs. 28.9 ± 2.0%, **p=0.0031) (Fig. 1A, Movies S1 and S2). These findings are similar to previous reports indicating that naive Teff cells have lower adhesion potential compared to naive Treg cells [36]. No significant difference was observed between adhesion of Teff cells and Treg cells after activation via their T cell receptor (TCR)/CD3ε (Fig. 1B, Movies S3 and S4) or addition of IL-2 along with TCR activation (Fig. 1C, Movies S5 and S6). The differential migratory potential of naïve Teff cells and Treg cells prompted us to study the effect of PDE8 inhibition using the PDE8 inhibitor PF-04957325 on motility of Teff and Treg cells.

3.2 PDE8 inhibition at the catalytic moiety leads to decreased adhesion of Teff cells but not Treg cells under shear flow conditions.

We have previously shown that PDE8A is differentially expressed in naive Teff cells versus naive Treg cells [23]. We now examined whether different expression levels of PDE8A can also be detected in pathogenic T cell populations involved in autoimmune inflammation. T cells were isolated at day 10 from draining lymph nodes of MOG_{35-55} immunized mice which is used to induce experimental autoimmune encephalomyelitis (EAE), a model for multiple sclerosis (MS) [37, 38]. $CD4^+CD25^-$ Teff cells showed significantly higher expression of PDE8A1 and PDE8A2 proteins compared to $CD4^+CD25^+$ Treg cells (Fig. 2A, B). There was no statistically significant difference in Raf-1 expression between the two cell populations (not shown). Next, we used *Foxp3gfp.KI* mice immunized with MOG_{35-55} to determine the effect of PDE8 inhibition on activated, pathogenic T cells. This approach enabled us to visually distinguish Teff and Treg cells and simultaneously measure the effect of inhibitors on Teff and Treg cells within the same experiment. PDE8 inhibition using 1 μM PF-04957325 led to a significant decrease in adhesion (100.0% vs. 63.3 ± 6.9%, **p=0.0019), and an increased trend of detachment, but this trend did not reach statistical significance (p=0.0510) of $CD4^+Foxp3^-GFP^-$ Teff cells compared to vehicle control treatment (Fig. 2C, Movies S7 and S8). No significant effect was observed on adhesion (100.0% vs. 108.6 ± 26.1%,

p=0.7536) and detachment (100.0% to 105.2± 9.1%, p=0.5850) of $CD4^+Foxp^+GFP^+$ Treg cells after PDE8 inhibition (Fig. 2D). The observed difference in PDE8A abundance between Teff and Treg cells could explain the differential effect of PDE8 inhibition on Teff cells vs. Treg cells in the flow assay.

3.3 Disruption of PDE8A-Raf-1 kinase signaling complex suppresses Teff and Treg cell adhesion.

PDE8A has been shown to interact with Raf-1 kinase without the need for accessory proteins or lipids and protect it from PKA mediated inhibitory phosphorylation. The Raf family members have been known to regulate adhesion of T cells to vascular ligands [28] We next used a cell permeable peptide that disrupts the PDE8A-Raf-1 interaction [19] to determine whether this complex regulates $CD4^+$ T cell motility under flow conditions. $CD4^+$ T cells isolated from draining lymph nodes of MOG_{35-55} immunized *Foxp3gfp.KI* mice and endothelial cells were treated with cell permeable disruptor or control peptides for 4 h. Treatment with the disruptor peptide decreased adhesion of $CD4^+GFP^-Foxp3^-$ Teff cells by 43.6 ± 14.3%, (100.0% vs. 56.4 ± 14.3%, *p= 0.0221). We also observed an increased trend of detachment, but this trend did not reach statistical significance (p=0.1919) (Fig.3A, Movies S9 and S10) compared to control. We also observed a decreased trend in adhesion of $CD4^+GFP^+Foxp3^+$ Treg cells, but this difference was not significant (p=0.1590) (Fig. 3B).

3.4 Adhesion, spreading and locomotion of Teff cells to ICAM-1 are significantly affected by disruption of the PDE8A-Raf-1 complex, but not by PDE8 inhibition at the catalytic moiety.

Next, we assessed whether PDE8 or the PDE8A-Raf-1 kinase complex regulate adhesion via LFA-1 integrin mediated cell tether formation with ICAM-1. For this purpose, we tested interaction of $CD4^+$ T cells on plates coated with recombinant ICAM-1-Fc protein under shear flow conditions. Treatment of $CD4^+$ T cells with PF-04957325 did not lead to significant differences in $CD4^+GFP^-Foxp3^-$ Teff cell mediated transient tethers (100.0% vs. 112.8 ± 53.0%, p=0.8213), firm tethers (100.0% vs. 99.8 ± 9.6%, p=0.9809), spreading (100.0% vs. 66.0 ± 28.8%, p=0.3038), locomotion (100.0% vs. 62.6 ± 29.6%, p=0.2744), detachment (100.0% vs.103.6 ± 2.3%, p=0.1944) (Fig. S1A), or adherence (100.0% vs. 68.6 ± 15.4%, p=0.1120) when ICAM-1 was used as a substrate in flow assays (Fig. 4A). There was also no significant effect of PF-04957325 treatment on $CD4^+GFP^+Foxp3^+$ Treg cell mediated firm tether formation (100.0% vs. 90.0 ± 13.2%, p=0.4916), adherence (100.0% vs. 191.5 ± 83.5%) or detachment (100.0% vs. 88.0 ± 6.7%, p=0.1498) (Fig. S1B). In contrast, treatment with the PDE8A-Raf-1 disruptor peptide led to a significant 52.6 ± 13.3% decrease in $CD4^+GFP^-Foxp3^-$ Teff cell adherence, (100.0% vs. 47.4 ± 13.3%, *p=0.0167), a significant 59.3 ± 4.3% decrease in spreading (100.0% vs. 40.7 ± 4.3%, *** p=0.0002) and a significant 72.7 ± 4.6% decrease in locomotion, (100.0% vs. 27.3 ± 4.6%, ****p < 0.0001) (Fig. 4B), but no significant effect was observed on transient tethers (100.0% vs. 150.8 ± 95.9%, p=0.6240), firm tethers (100.0% vs. 60.3 ± 23.3%, p=0.1634) and detachment (100.0% vs. 106.1 ± 3.6% p=0.1688)

of Teff cells when ICAM-1 was used as a substrate (Fig. S1C, Movies S11 and S12). Of note, there was also a significant 43.3 ± 13.1% decrease in adherent cell tethers of $CD4^+GFP^+Foxp3^+$ Treg cells interacting with ICAM-1 (100.0% vs. 56.7 ± 13.1%, *p=0.0299) after treatment with the disruptor peptide (Fig. 4C). No significant effect on firm tether formation (100.0% vs. 65.5 ± 25.3%, p=0.2450) and detachment (100.0% vs. 112.9 ± 9.3%, p=0.2358) of Treg cells was observed (Fig. S1D). These data implicate the LFA-1-ICAM-1 interaction as a target of PDE8A-Raf-1 kinase complex disruption.

3.5 $CD4^+$ T cell mediated firm cell tether formation to VCAM-1 is unaffected by disruption of PDE8A-Raf-1 complex and PDE8 inhibition at the catalytic moiety.

To further explore whether the effect of the PDE8 inhibitor or the PDE8A-Raf-1 complex disruptor peptide on adhesion of $CD4^+$ T cells was dependent on the integrin VLA-4, we tested binding of cells to its selective ligand, VCAM-1 under flow [39]. No significant differences were observed in transient tethers, (100.0% vs. 196.1 ± 81.9%, p=0.2849), rolling (100.0% vs. 87.6 ± 23.8%, p=0.6204), firm tethers (100.0% vs. 134.7 ± 36.6%, p=0.3805), adherence (100.0% vs. 127.9 ± 48.8%, p=0.5881) and detachment (100.0% vs. 99.8 ± 0.6%, p=0.7070) in $CD4^+$ T cell interaction with VCAM-1 after treatment with PDE8 inhibitor (Fig. S2A). Treatment with disruptor peptide did not have any significant effect on transient tethers (100.0% vs. 90.4 ± 22.7%, p=0.6860), firm tethers (100.0% vs. 81.2 ± 13.3%, p=0.2074), adherence (100.0% to 69.5 ± 23.4%, p=0.2402) and detachment (100.0% vs. 102.5 ± 1.7%, p=0.1967). However, there was a significant 56.4 ± 7.3% suppression of rolling (100.0% vs. 43.6 ± 7.3%, **p=0.0015) after treatment with the disruptor peptide, indicating a selective effect of the peptide on initial loose tethers of T cells to VCAM-1 (Fig. S2B).

3.6 Integrin surface expression in $CD4^+$ T cells is not altered by PDE8 inhibition at the catalytic moiety and marginally reduced by disruption of the PDE8A-Raf-1 complex.

α4 and αL integrins as well as CD44 are known cell surface molecules regulating myelin antigen specific Teff cell migration into the central nervous system [30, 31] and are targets of drug therapies [40]. We tested the effect of the PDE8 inhibitor and the disruptor peptide on the surface expression of these adhesion molecules by flow cytometry. PF-04957325 treatment did not significantly alter the mean fluorescence intensity (MFI) of αL integrin (p=0.2608), α4 integrin (p=0.1053) or CD44 (p=0.3675) in $CD4^+Foxp3^-GFP^-$ Teff cells (Fig. S3A) or $CD4^+GFP^+Foxp3^+$ Treg cells (p=0.5396; p=0.0677; p=0.0899, respectively; Fig. S3B). In contrast, there was a small but significant 2830 ± 645.8 unit decrease in the MFI of αL integrin expression (30957 ± 350.1 vs. 28127 ± 542.7, *p=0.0119) and a 259.7 ± 65.19 units decrease in MFI of CD44 expression (3453 ± 55.98 vs. 3194 ± 33.39, *p=0.0164) but not in MFI of α4 integrin (p=0.3814) in $CD4^+Foxp3^-GFP^-$ Teff cells after treatment with the disruptor peptide (Fig. S3A). Disruptor peptide treatment did not significantly alter MFI of αL integrin (p=0.1025), α4 integrin (p=0.8069) or

CD44 (p=0.0573) in $CD4^+GFP^+Foxp3^+$ Treg cells. Of note, PF-04957325 and disruptor peptide treatments did not affect the viability of $CD4^+$ T cells (Fig. S4)

3.7 PDE8 inhibition at the catalytic moiety significantly suppresses ERK phosphorylation in $CD4^+$ T cells activated by anti-CD3.

To find out whether the effect of the PDE8 and PDE8A-Raf-1 complex inhibition on $CD4^+$ T cell motility directly affects Raf-1 or ERK signaling, we performed assays to determine inhibitory phosphorylation of Raf-1 at S259 and activating phosphorylation of ERK1/2 after treatment and activation through the TCR. ERK1/2 phosphorylation (Thr202/Tyr204) and Raf-1 phosphorylation (S259) was analyzed by Western blot (Fig. 5). We observed no significant effect on Raf-1 phosphorylation (100.0% vs. 104.3 ± 7.2%, p=0.5937), but a significant 36.2 ± 6.8% decrease in ERK1 phosphorylation (100.0% vs. 63.8 ± 6.2%, ***p=0.0002) and a significant 27.9 ± 9.366% decrease in ERK2 phosphorylation (100.0% vs. 72.1 ± 8.6%, *p=0.0125) in $CD4^+$ T cells after 1 h treatment with PF-04957325 compared to the vehicle control (Fig. 5A,B). These results indicate that the PDE8 enzyme regulates in part the ERK1/2 signaling pathway. We also report that inhibition of PDE8 enzymatic activity led to a 71.4 ± 25.8% compensatory increase in PDE8A protein expression, (100.0% vs. 171.4 ± 23.7%, *p=0.0183) (Fig. 5C-D). Augmentation of PDE7A, PDE3B, PDE4B and PDE4D expression after treatment with cAMP elevating agents or gene family specific PDE inhibitors has been reported before [41-43], and we show here that this occurs with PDE8A as well.

3.8 Disruption of the PDE8A-Raf-1 complex increases inhibitory Raf-1 phosphorylation and activating ERK1/2 phosphorylation in $CD4^+$ T cells activated by anti-CD3.

Treatment with the disruptor peptide for 1 h followed by 15 min anti-CD3 stimulation led to a 32.17 ± 8% decrease of ERK1 phosphorylation (100% to 67.8 ± 7.3%, **p=0.0020) and a 23.6 ± 6.3% decrease in ERK2 phosphorylation, (100% to 76.4 ± 5.8 %, ** p=0.0033), but had no significant effect on PKA mediated inhibitory Raf-1 phosphorylation (100% vs. 111 ± 11.5%, p=0.3572) compared to the control treatment (Fig. 6A-B). In a kinetic study beyond the 1 h time point (Fig. 6A,C-D), treatment with the PDE8A-Raf-1 disruptor peptide for 2 h and 4 h led to a 38.9 ± 22% (100% vs. 138.9 ± 22%, p=0.1283) and 100.4 ± 40.5% (100% vs. 200.4 ± 40.5%, *p=0.0264) increase in Raf-1 phosphorylation, respectively. Additionally, there was an 67.8 ± 20.4% increase at 2 h (100% vs. 167.9 ± 20.4%, *p=0.0158) and a 201.3 ± 53.3% increase at 4 h (100% vs. 301.3 ± 49.6%, **p=0.0023) in ERK1 phosphorylation and a 33.2 ± 13% increase at 2 h (100% vs.133.2 ± 13%, *p=0.0438) and a 184.6 ± 49.5% increase at 4 h (100% vs. 284.6 ± 46.1%, *p=0.0025) in ERK2 phosphorylation in $CD4^+$ T cells exposed to the disruptor peptide. Since in flow assays the $CD4^+$ T cells were treated with the peptide for 4 h, our data indicate that the major effect of the PDE8A-Raf-1 complex is dependent on Raf-1 signaling independent of the downstream ERK-MAPK pathway. Despite this robust effect on inhibitory Raf-1 phosphorylation, treatment with the PDE8A-Raf-1 disruptor peptide for 4 h leads to an increase of

activating ERK1/2 phosphorylation that could be mediated by a large number of effectors acting through ERK during T cell activation [44].

4. Discussion

Previous work has shown that PDE8A is expressed in activated $CD4^+$ T cells [5, 6, 22, 23]. Functionally, we have reported that PDE8 regulates T cell motility as inhibition of PDE8 is a non-redundant means to suppress lymphocyte chemotaxis and adhesion [6, 22, 24]. Moreover, we have recently shown that PDE8A is expressed in breast cancer cell lines and inhibition of PDE8 suppresses breast cancer cell migration [21]. These previously described roles of PDE8 in cell motility prompted us to mechanistically investigate the specific cell migration categories and molecular signaling complexes that are regulated by PDE8.

PDEs control intracellular cAMP gradients and are positioned in discrete signaling complexes. Much is known about spatial arrangements and specific functions of some PDE isoforms such as PDE4 [45-47]. Much of this knowledge has stemmed from the use of disruptor peptides that have no effect on global PDE activity but can discretely displace small pools of tethered PDE from precise microdomains. For example, PDE4D5 forms signaling complexes with signaling and adhesion molecules that regulate spreading of cancer cells [48] and endothelial inflammation [49]. A dearth of information, however, exists for complexes involving PDE8A. A recent study by Baillie and colleagues demonstrated the first such PDE8 specific signaling complex [19]. In this study, we addressed a major gap in the literature by delineating the parts of the mechanism by which PDE8 inhibition acts in T cells, and by investigating the function of the PDE8A-Raf-1 complex in T cells. To analyze T cell migration under physiological conditions, we did motility assays under shear flow conditions. To delineate the role of PDE8 in different T cell populations involved in pro- and antiinflammatory immune responses, we subjected polyclonal and antigen-activated Teff and Treg cells to physiological shear stress in flow chamber assays. Our results indicate the higher adhesion of naive Treg cells compared to naive Teff cells. Further activation of these cells with plate bound anti-CD3 led to an increase in migratory potential of Teff cells, comparable to the Treg cells. Our results indicate that enzymatic inhibition of PDE8 using the specific PDE8 inhibitor, PF-04957325, leads to significant reduction of Teff cell adhesion. In contrast, Treg motility is not significantly affected by PDE8 inhibition. This differential effect on both the cell populations is consistent with the observed differential expression of PDE8A in Teff cells versus Treg cells where it is considerably more highly expressed in Teff cells. Treatment with the PDE8A-Raf-1 disruptor peptide had a more potent effect on Teff cell adhesion, which suggested the specific involvement of the PDE8A-Raf-1 signaling complex in the control of $CD4^+$ T cell motility beyond a role for the global pool of PDE8 in T cells. Although it was shown that the disruptor peptide clearly inhibits Raf-1 binding to PDE8, it remains a concern that the disruptor peptide might possibly also inhibit the binding of Raf-1 to other proteins. However, it is noteworthy that

overexpression of a catalytically inactive mutant form of PDE8A displayed a dominant negative phenotype and recapitulated the effects of treatment of cells with the disruptor peptide, as did mice and Drosophila genetically modified to knock out PDE8A [19]**.** Inasmuch as these treatments mimicked the effects of disruptor peptide treatment on ERK activation and sensitization to stress-induced death, it at least suggests that the primary action of disruptor peptide is to disrupt the binding of Raf-1 from PDE8A, rather than from an association with other protein(s), which otherwise would not have been reproduced by dominant negative PDE8A overexpression and knockout of PDE8A in the germline.

In order to dissect the molecular mechanism by which PDE8 and the PDE8A-Raf-1 complex regulate adhesion, we further tested the effect of the enzymatic inhibitor and signaling complex disruptor on interaction of activated $CD4^+$ T cells isolated from lymph nodes of mice immunized with MOG_{35-55}/CFA with endothelial ligands, VCAM-1 and ICAM-1, molecules critically involved in inflammation [40]. Treatment with the disruptor peptide led to a significant reduction in firm adhesion, spreading and locomotion of Teff cells as well as reduction in firm adhesion of Treg cells while interacting with ICAM-1. Thus PDE8A-Raf-1 signaling complex regulates LFA-1 integrin mediated tether formation while interacting with ICAM-1 vascular adhesion molecules. The expression of αL, α4 integrin and CD44 expression in $CD4^+Foxp3^-GFP^-$ Teff cells and $CD4^+Foxp3^+GFP^+$ Treg cells after treatment with the PDE8 enzymatic inhibitor or the complex disruptor peptide was marginally reduced or unaltered suggesting that the effect on adhesion was dependent on adhesion molecule activation or coupling to the cytoskeleton rather than cell surface expression (Fig. S3A, B) [28, 32, 33]. Importantly, neither PF-04957325 nor disruptor peptide treatment affected the viability of cells exposed to doses and for time periods identical to those used in functional assays (Fig. S4).

While most observed effects of disruptor peptide were recapitulated by treatment with the PDE8-selective inhibitor, the effects of disruptor peptide were more pronounced on some, such as adhesion to ICAM-1. We are not certain why this difference exists in the potency of disruptor peptide as compared to PF-04957325, but this may simply be a reflection of the different ways in which these two treatments are acting. Whereas disruptor peptide dissociates PDE8A from the signalosome complex and alters its localization in the cell such that it can no longer regulate the pool of cAMP associated with regulating phosphorylation of Raf-1, the PDE8-selective inhibitor, PF-04957325, must act to inhibit the catalytic activity of PDE8A. One can never be certain that treatment of intact cells with an enzyme inhibitor can fully inhibit that enzyme's activity, as the capacity to inhibit the target enzyme can be greatly influenced by how much of the inhibitor gets into the cell, and how it distributes in the cell. Further, since the PDE8A remains bound to Raf-1 in the signalosome complex upon treatment with PF-04957325, it is possible that PF-04957325 may not gain full access to the catalytic site of PDE8A while it is complexed with these other proteins. Another explanation may lie in the selectivity of disrupting a limited signaling complex containing just

PDE8A versus inhibiting a potentially large number of PDE8 molecules, including PDE8A and 8B distributed throughout the cell. Since cell motility is tightly regulated in opposing directions by specific signaling pathways, it is possible that PF-04957325 acts on PDE8 acting in both adhesion activating and inhibiting signaling complexes. The net effect of a small molecule inhibitor could thus be quite different from the effect of a specific complex disruptor.

It is noteworthy that our data suggest a Raf-1 dependent but ERK independent effect of PDE8 inhibition on T cell motility as disruption of the PDE8A-Raf-1 complex through the disruptor peptide led to inhibitory phosphorylation of Raf-1 while activating ERK1/2. Previous reports implicate Raf-1 and B-Raf in regulating migration by controlling Rho GTPase mediated downstream signaling which regulates actin cytoskeletal and focal adhesion dynamics [50, 51]. Our findings further confirm the role of Raf-1 in regulating this process and point towards existence of the novel signaling complex regulating $CD4^+$ T cell motility. Raf-1 is the major downstream effector linking TCR mediated Ras activation to MEK1/2 and ERK1/2 [44]. However, B-Raf has been identified as the most efficient in interacting with Ras [52, 53] and in activating ERK [54-56]. Importantly, ERK activation and cell proliferation can proceed independently of Raf-1, while Raf-1 can regulate the Rho downstream signaling during cell migration independently of ERK signaling [51], highlighting the independent regulation and function of these MAPKs in different signaling pathways. Importantly, in T cells, TCR stimulation can also lead to Ras/Raf-1-independent activation of ERK [44]. Moreover, findings that PDE8 inhibition has little effect on T cell proliferation [6, 24] indicates an ERK independent action. In contrast, PDE4 inhibition profoundly inhibits cell proliferation and ERK1/2 signaling [57], but has little effect on T cell motility [24, 58]. Taken together, our findings that inhibition of PDE8 and the PDE8A-Raf-1 signaling complex leads to suppression of T cell motility in the absence of marked inhibition of proliferation indicates a novel role for a pool of PDE8A regulating Raf-1 kinase independently of downstream ERK1/2 signaling.

5. Conclusions

This study demonstrates for the first time that T cell motility under physiological shear stress conditions is profoundly modulated by a pool of PDE8A. This effect is mediated by the interaction between PDE8A and Raf-1 kinase and constitutes a novel signaling axis for the investigation of T cell adhesion and migration.

Acknowledgements
We thank Pfizer Inc. for providing PF-04957325 through the CTP. We are grateful to Dr. Frank Menniti for his advice and discussions. This investigation was supported by the National Multiple Sclerosis Society (grant RG 4544A1/1), the Smart Family Foundation and Lea's Foundation for Leukemia Research Inc.

Figure Legends

Fig. 1: Differential motility of naive and *in vitro* activated $CD4^+$ Teff and Treg cells while interacting with endothelial cell monolayers under shear stress conditions.

Adhesion of $CD4^+CD25^-$ Teff cells and $CD4^+CD25^+$ Treg cells isolated from spleens assayed under shear stress conditions (5 dyn/cm^2): (A) naive (for naive Teff and naive Treg cell flow assays: n=4, 2 independent experiments), (B) anti-CD3 stimulation for 18 h (for anti-CD3 activated Teff cell assays: n=5, 3 independent experiments; anti-CD3 activated Treg cell assays: n=7, 6 independent experiments) and (C) anti-CD3 + IL-2 for 18 h (anti-CD3 + IL-2 Teff cell assays: n=7, 3 independent experiments; anti-CD3 + IL-2 Treg cell assays: n=5, 3 independent experiments). Data (mean ± SEM) are expressed as percentage out of total cells present in the flow chamber before the start of flow.

Fig. 2: PDE8 inhibition at the catalytic moiety suppresses $CD4^+$ Teff cell motility but not Treg cell motility.

(A) The immunoblot shows PDE8A1 and PDE8A2 expression of *in vivo* MOG_{35-55} activated $CD4^+CD25^-$ Teff and $CD4^+CD25^+$ Treg cells isolated from the draining PLNs on day 10 post immunization. (B) Relative PDE8A1 and PDE8A2 expression normalized to GAPDH. Data are from T cells isolated from lymph nodes pooled from 5 mice. Data represent mean ± SEM from 3 independent experiments. (C, D) LPS activated endothelial cells and MOG_{35-55} primed $CD4^+$ T cells were treated with either vehicle or 1 μM PF-04957325 for 1 h. Adhesion and detachment of $CD4^+Foxp3^-GFP^-$ Teff cells (C) and $CD4^+Foxp3^+GFP^+$ Treg cells (D) were analyzed under shear stress. Data represent mean ± SEM results from 4 independent experiments and are expressed as percentage of total cells that accumulate in the flow chamber before the flow starts. Percentage of cells in each category is normalized to the vehicle condition set at 100 percent.

Fig. 3: Disruption of the PDE8A-Raf-1 complex suppresses both $CD4^+$ Teff and Treg cell motility.

LPS activated endothelial cells and MOG_{35-55} primed $CD4^+$ T cells isolated from the draining PLNs on day 10 post immunization were treated with either 10 μM scrambled (control) peptide or disruptor peptide for 4 h. Adhesion and detachment of $CD4^+Foxp3^-GFP^-$ Teff cells (A) and $CD4^+Foxp3^+GFP^+$ Treg cells (B) were analyzed under shear stress. Data represent mean ± SEM results from 3-4 independent experiments and are expressed as percentage of total cells that accumulate in the flow chamber before the flow starts. Percentage of cells in each category is normalized to the vehicle condition set at 100 percent.

Fig. 4: Adhesiveness to ICAM-1 significantly affected by disruption of the PDE8A-Raf-1 complex, but not by PDE8 inhibition at the catalytic moiety.

MOG_{35-55} primed $CD4^+$ T cells isolated from the draining PLNs on day 10 post immunization were treated with vehicle or 1 μM PDE8 inhibitor for 1 h (A) or 10 μM control peptide or disruptor peptide for 4 h (B, C). Spontaneous tethering

(adherent cells, spreading or locomotion) of the $CD4^+Foxp3^-GFP^-$ Teff cells (A, B) and $CD4^+Foxp3^+GFP^+$ Treg cells (C) while interacting with high density ICAM-1-Fc (5 µg/ml) were analyzed under flow. Data represent mean ± SEM results from 3 independent experiments and are expressed as percentage of total cells that accumulate in the flow chamber before the flow starts. Percentage of cells in each category is normalized to the vehicle condition set at 100 percent.

Fig. 5: Inhibition of PDE8 in $CD4^+$ T cells diminishes ERK1/2 phosphorylation induced by CD3.
MOG_{35-55} primed $CD4^+$ T cells isolated from the draining PLNs on day 10 post-immunization were treated with vehicle or 1 µM PF-04957325 for 1 h followed by anti-CD3 stimulation for 15 min. Cell lysates were then probed for (A) phospho Raf-1 (S259), Raf-1, phospho ERK1/2, ERK1/2, (C) PDE8A1 and GAPDH by Western blot. (B, D) Bands were quantitated by densitometry and data are presented as phospho-Raf-1 (S259) relative to Raf-1, phospho-ERK1/2 relative to ERK1/2 and PDE8A1 expression relative to GAPDH. Data represent mean ± SEM results from 4 independent experiments (n=7).

Fig. 6: Disruption of the PDE8A-Raf-1 complex in $CD4^+$ T cells increases inhibitory Raf-1 phosphorylation at serine 259 and increases ERK1/2 phosphorylation induced by CD3.
MOG_{35-55} primed $CD4^+$ T cells isolated from the draining PLNs on day 10 post-immunization were treated with 10 µM control peptide (CP) or disruptor peptide (DP) for 1 h (A, B), 2 h (A, C) and 4 h (A, D) followed by anti-CD3 stimulation for 15 min. Cell lysates were then probed for phospho Raf-1 (S259), Raf-1, phospho ERK1/2, ERK1/2 and GAPDH by Western blot. (B-D) Bands were quantitated by densitometry and data are presented as phospho-Raf-1 (S259) relative to Raf-1 and phospho-ERK1/2 relative to ERK1/2 at 1, 2 and 4 h. Data represent mean ± SEM from 2 independent experiments (n=5).

References

[1] J.A. Ledbetter, M. Parsons, P.J. Martin, J.A. Hansen, P.S. Rabinovitch, C.H. June, Antibody binding to CD5 (Tp67) and Tp44 T cell surface molecules: effects on cyclic nucleotides, cytoplasmic free calcium, and cAMP-mediated suppression, J Immunol, 137 (1986) 3299-3305.
[2] T. Wang, J.R. Sheppard, J.E. Foker, Rise and fall of cyclic AMP required for onset of lymphocyte DNA synthesis, Science, 201 (1978) 155-157.
[3] B.S. Skalhegg, B.F. Landmark, S.O. Doskeland, V. Hansson, T. Lea, T. Jahnsen, Cyclic AMP-dependent protein kinase type I mediates the inhibitory effects of 3',5'-cyclic adenosine monophosphate on cell replication in human T lymphocytes, J Biol Chem, 267 (1992) 15707-15714.
[4] L. Li, C. Yee, J.A. Beavo, CD3- and CD28-dependent induction of PDE7 required for T cell activation, Science, 283 (1999) 848-851.
[5] N.A. Glavas, C. Ostenson, J.B. Schaefer, V. Vasta, J.A. Beavo, T cell activation up-regulates cyclic nucleotide phosphodiesterases 8A1 and 7A3, Proc Natl Acad Sci U S A, 98 (2001) 6319-6324.
[6] A.G. Vang, S.Z. Ben-Sasson, H. Dong, B. Kream, M.P. DeNinno, M.M. Claffey, W. Housley, R.B. Clark, P.M. Epstein, S. Brocke, PDE8 regulates rapid Teff cell adhesion and proliferation independent of ICER, PLoS One, 5 (2010) e12011.
[7] M.A. Giembycz, C.J. Corrigan, J. Seybold, R. Newton, P.J. Barnes, Identification of cyclic AMP phosphodiesterases 3, 4 and 7 in human CD4+ and CD8+ T-lymphocytes: role in regulating proliferation and the biosynthesis of interleukin-2, Br J Pharmacol, 118 (1996) 1945-1958.
[8] H. Tenor, L. Staniciu, C. Schudt, A. Hatzelmann, A. Wendel, R. Djukanovic, M.K. Church, J.K. Shute, Cyclic nucleotide phosphodiesterases from purified human CD4+ and CD8+ T lymphocytes, Clin Exp Allergy, 25 (1995) 616-624.
[9] S. Yoon, R. Seger, The extracellular signal-regulated kinase: multiple substrates regulate diverse cellular functions, Growth Factors, 24 (2006) 21-44.
[10] S. Vallabhapurapu, M. Karin, Regulation and function of NF-kappaB transcription factors in the immune system, Annu Rev Immunol, 27 (2009) 693-733.
[11] L. Chang, M. Karin, Mammalian MAP kinase signalling cascades, Nature, 410 (2001) 37-40.
[12] M. Cargnello, P.P. Roux, Activation and function of the MAPKs and their substrates, the MAPK-activated protein kinases, Microbiol Mol Biol Rev, 75 (2011) 50-83.
[13] I. Merida, E. Andrada, S.I. Gharbi, A. Avila-Flores, Redundant and specialized roles for diacylglycerol kinases alpha and zeta in the control of T cell functions, Sci Signal, 8 (2015) re6.
[14] H. Lavoie, M. Therrien, Regulation of RAF protein kinases in ERK signalling, Nat Rev Mol Cell Biol, 16 (2015) 281-298.
[15] N. Dumaz, R. Marais, Protein kinase A blocks Raf-1 activity by stimulating 14-3-3 binding and blocking Raf-1 interaction with Ras, J Biol Chem, 278 (2003) 29819-29823.

[16] A.S. Dhillon, W. Kolch, Untying the regulation of the Raf-1 kinase, Arch Biochem Biophys, 404 (2002) 3-9.
[17] A.S. Dhillon, C. Pollock, H. Steen, P.E. Shaw, H. Mischak, W. Kolch, Cyclic AMP-dependent kinase regulates Raf-1 kinase mainly by phosphorylation of serine 259, Mol Cell Biol, 22 (2002) 3237-3246.
[18] D.H. Maurice, PDE8A runs interference to limit PKA inhibition of Raf-1, Proc Natl Acad Sci U S A, 110 (2013) 6248-6249.
[19] K.M. Brown, J.P. Day, E. Huston, B. Zimmermann, K. Hampel, F. Christian, D. Romano, S. Terhzaz, L.C. Lee, M.J. Willis, D.B. Morton, J.A. Beavo, M. Shimizu-Albergine, S.A. Davies, W. Kolch, M.D. Houslay, G.S. Baillie, Phosphodiesterase-8A binds to and regulates Raf-1 kinase, Proc Natl Acad Sci U S A, 110 (2013) E1533-1542.
[20] K.M. Brown, L.C. Lee, J.E. Findlay, J.P. Day, G.S. Baillie, Cyclic AMP-specific phosphodiesterase, PDE8A1, is activated by protein kinase A-mediated phosphorylation, FEBS Lett, 586 (2012) 1631-1637.
[21] H. Dong, K.P. Claffey, S. Brocke, P.M. Epstein, Inhibition of breast cancer cell migration by activation of cAMP signaling, Breast cancer research and treatment, 152 (2015) 17-28.
[22] H. Dong, V. Osmanova, P.M. Epstein, S. Brocke, Phosphodiesterase 8 (PDE8) regulates chemotaxis of activated lymphocytes, Biochem Biophys Res Commun, 345 (2006) 713-719.
[23] A.G. Vang, W. Housley, H. Dong, C. Basole, S.Z. Ben-Sasson, B.E. Kream, P.M. Epstein, R.B. Clark, S. Brocke, Regulatory T-cells and cAMP suppress effector T-cells independently of PKA-CREM/ICER: a potential role for Epac, Biochem J, 456 (2013) 463-473.
[24] A.G. Vang, C. Basole, H. Dong, R.K. Nguyen, W. Housley, L. Guernsey, A.J. Adami, R.S. Thrall, R.B. Clark, P.M. Epstein, S. Brocke, Differential Expression and Function of PDE8 and PDE4 in Effector T cells: Implications for PDE8 as a Drug Target in Inflammation, Front Pharmacol, 7 (2016) 259.
[25] H. Wang, Z. Yan, S. Yang, J. Cai, H. Robinson, H. Ke, Kinetic and structural studies of phosphodiesterase-8A and implication on the inhibitor selectivity, Biochemistry, 47 (2008) 12760-12768.
[26] V. Vasta, cAMP-Phosphodiesterase 8 Family, in: J.A. Beavo, S.H. Francis, M.D. Houslay (Eds.) Cyclic Nucleotide Phosphodiesterases in Health and Disease, CRC press, New York, NY, 2007, pp. 205-219.
[27] P.M. Epstein, J.S. Mills, E.M. Hersh, S.J. Strada, W.J. Thompson, Activation of cyclic nucleotide phosphodiesterase from isolated human peripheral blood lymphocytes by mitogenic agents, Cancer Res, 40 (1980) 379-386.
[28] W.S. Brown, J.S. Khalili, T.G. Rodriguez-Cruz, G. Lizee, B.W. McIntyre, B-Raf regulation of integrin alpha4beta1-mediated resistance to shear stress through changes in cell spreading and cytoskeletal association in T cells, J Biol Chem, 289 (2014) 23141-23153.
[29] T. Korn, J. Reddy, W. Gao, E. Bettelli, A. Awasthi, T.R. Petersen, B.T. Backstrom, R.A. Sobel, K.W. Wucherpfennig, T.B. Strom, M. Oukka, V.K. Kuchroo, Myelin-specific regulatory T cells accumulate in the CNS but fail to control autoimmune inflammation, Nat Med, 13 (2007) 423-431.

[30] T.A. Yednock, C. Cannon, L.C. Fritz, F. Sanchez-Madrid, L. Steinman, N. Karin, Prevention of experimental autoimmune encephalomyelitis by antibodies against alpha 4 beta 1 integrin, Nature, 356 (1992) 63-66.
[31] S. Brocke, C. Piercy, L. Steinman, I.L. Weissman, T. Veromaa, Antibodies to CD44 and integrin alpha4, but not L-selectin, prevent central nervous system inflammation and experimental encephalomyelitis by blocking secondary leukocyte recruitment, Proc Natl Acad Sci U S A, 96 (1999) 6896-6901.
[32] Z. Shulman, R. Alon, Chapter 14. Real-time in vitro assays for studying the role of chemokines in lymphocyte transendothelial migration under physiologic flow conditions, Methods Enzymol, 461 (2009) 311-332.
[33] S.W. Feigelson, R. Pasvolsky, S. Cemerski, Z. Shulman, V. Grabovsky, T. Ilani, A. Sagiv, F. Lemaitre, C. Laudanna, A.S. Shaw, R. Alon, Occupancy of lymphocyte LFA-1 by surface-immobilized ICAM-1 is critical for TCR- but not for chemokine-triggered LFA-1 conversion to an open headpiece high-affinity state, J Immunol, 185 (2010) 7394-7404.
[34] S.W. Feigelson, V. Grabovsky, E. Manevich-Mendelson, R. Pasvolsky, Z. Shulman, V. Shinder, E. Klein, A. Etzioni, M. Aker, R. Alon, Kindlin-3 is required for the stabilization of TCR-stimulated LFA-1:ICAM-1 bonds critical for lymphocyte arrest and spreading on dendritic cells, Blood, 117 (2011) 7042-7052.
[35] M.A. Gavin, J.P. Rasmussen, J.D. Fontenot, V. Vasta, V.C. Manganiello, J.A. Beavo, A.Y. Rudensky, Foxp3-dependent programme of regulatory T-cell differentiation, Nature, 445 (2007) 771-775.
[36] E. Maganto-Garcia, D.X. Bu, M.L. Tarrio, P. Alcaide, G. Newton, G.K. Griffin, K.J. Croce, F.W. Luscinskas, A.H. Lichtman, N. Grabie, Foxp3+-inducible regulatory T cells suppress endothelial activation and leukocyte recruitment, J Immunol, 187 (2011) 3521-3529.
[37] A. Biton, S. Ansorge, U. Bank, M. Tager, D. Reinhold, S. Brocke, Divergent actions by inhibitors of DP IV and APN family enzymes on CD4+ Teff cell motility and functions, Immunobiology, 216 (2011) 1295-1301.
[38] S. Brocke, L. Quigley, H.F. McFarland, L. Steinman, Isolation and Characterization of Autoreactive T Cells in Experimental Autoimmune Encephalomyelitis of the Mouse, Methods, 9 (1996) 458-462.
[39] E. Manevich-Mendelson, S.W. Feigelson, R. Pasvolsky, M. Aker, V. Grabovsky, Z. Shulman, S.S. Kilic, M.A. Rosenthal-Allieri, S. Ben-Dor, A. Mory, A. Bernard, M. Moser, A. Etzioni, R. Alon, Loss of Kindlin-3 in LAD-III eliminates LFA-1 but not VLA-4 adhesiveness developed under shear flow conditions, Blood, 114 (2009) 2344-2353.
[40] L. Steinman, The discovery of natalizumab, a potent therapeutic for multiple sclerosis, J Cell Biol, 199 (2012) 413-416.
[41] R. Lee, S. Wolda, E. Moon, J. Esselstyn, C. Hertel, A. Lerner, PDE7A is expressed in human B-lymphocytes and is up-regulated by elevation of intracellular cAMP, Cell Signal, 14 (2002) 277-284.
[42] E. Moon, R. Lee, R. Near, L. Weintraub, S. Wolda, A. Lerner, Inhibition of PDE3B augments PDE4 inhibitor-induced apoptosis in a subset of patients with chronic lymphocytic leukemia, Clin Cancer Res, 8 (2002) 589-595.

[43] X. Jiang, M. Paskind, R. Weltzien, P.M. Epstein, Expression and regulation of mRNA for distinct isoforms of cAMP-specific PDE-4 in mitogen-stimulated and leukemic human lymphocytes, Cell Biochem Biophys, 28 (1998) 135-160.
[44] R.L. Kortum, A.K. Rouquette-Jazdanian, L.E. Samelson, Ras and extracellular signal-regulated kinase signaling in thymocytes and T cells, Trends Immunol, 34 (2013) 259-268.
[45] G.S. Baillie, J.D. Scott, M.D. Houslay, Compartmentalisation of phosphodiesterases and protein kinase A: opposites attract, FEBS Lett, 579 (2005) 3264-3270.
[46] H. Abrahamsen, G. Baillie, J. Ngai, T. Vang, K. Nika, A. Ruppelt, T. Mustelin, M. Zaccolo, M. Houslay, K. Tasken, TCR- and CD28-mediated recruitment of phosphodiesterase 4 to lipid rafts potentiates TCR signaling, J Immunol, 173 (2004) 4847-4858.
[47] G.S. Baillie, Compartmentalized signalling: spatial regulation of cAMP by the action of compartmentalized phosphodiesterases, FEBS J, 276 (2009) 1790-1799.
[48] B. Serrels, E. Sandilands, A. Serrels, G. Baillie, M.D. Houslay, V.G. Brunton, M. Canel, L.M. Machesky, K.I. Anderson, M.C. Frame, A complex between FAK, RACK1, and PDE4D5 controls spreading initiation and cancer cell polarity, Curr Biol, 20 (2010) 1086-1092.
[49] S. Yun, M. Budatha, J.E. Dahlman, B.G. Coon, R.T. Cameron, R. Langer, D.G. Anderson, G. Baillie, M.A. Schwartz, Interaction between integrin alpha5 and PDE4D regulates endothelial inflammatory signalling, Nat Cell Biol, 18 (2016) 1043-1053.
[50] R.M. Klein, L.S. Spofford, E.V. Abel, A. Ortiz, A.E. Aplin, B-RAF regulation of Rnd3 participates in actin cytoskeletal and focal adhesion organization, Mol Biol Cell, 19 (2008) 498-508.
[51] K. Ehrenreiter, D. Piazzolla, V. Velamoor, I. Sobczak, J.V. Small, J. Takeda, T. Leung, M. Baccarini, Raf-1 regulates Rho signaling and cell migration, J Cell Biol, 168 (2005) 955-964.
[52] R. Marais, Y. Light, H.F. Paterson, C.S. Mason, C.J. Marshall, Differential regulation of Raf-1, A-Raf, and B-Raf by oncogenic ras and tyrosine kinases, J Biol Chem, 272 (1997) 4378-4383.
[53] C.K. Weber, J.R. Slupsky, C. Herrmann, M. Schuler, U.R. Rapp, C. Block, Mitogenic signaling of Ras is regulated by differential interaction with Raf isozymes, Oncogene, 19 (2000) 169-176.
[54] C.A. Pritchard, L. Hayes, L. Wojnowski, A. Zimmer, R.M. Marais, J.C. Norman, B-Raf acts via the ROCKII/LIMK/cofilin pathway to maintain actin stress fibers in fibroblasts, Mol Cell Biol, 24 (2004) 5937-5952.
[55] C.A. Pritchard, M.L. Samuels, E. Bosch, M. McMahon, Conditionally oncogenic forms of the A-Raf and B-Raf protein kinases display different biological and biochemical properties in NIH 3T3 cells, Mol Cell Biol, 15 (1995) 6430-6442.
[56] L. Wojnowski, L.F. Stancato, A.C. Larner, U.R. Rapp, A. Zimmer, Overlapping and specific functions of Braf and Craf-1 proto-oncogenes during mouse embryogenesis, Mech Dev, 91 (2000) 97-104.

[57] A. Norambuena, C. Metz, L. Vicuna, A. Silva, E. Pardo, C. Oyanadel, L. Massardo, A. Gonzalez, A. Soza, Galectin-8 induces apoptosis in Jurkat T cells by phosphatidic acid-mediated ERK1/2 activation supported by protein kinase A down-regulation, J Biol Chem, 284 (2009) 12670-12679.
[58] A. Lerner, P.M. Epstein, Cyclic nucleotide phosphodiesterases as targets for treatment of haematological malignancies, Biochem J, 393 (2006) 21-41.

Supporting Information

Figure Legends

Fig. S1: Adhesiveness to ICAM-1 significantly affected by disruption of the PDE8A-Raf-1 complex, but not by PDE8 inhibition at the catalytic moiety.
MOG_{35-55} primed $CD4^+$ T cells isolated from the draining PLNs on day 10 post-immunization were treated with vehicle or 1 μM PDE8 inhibitor for 1 h (A, B) or 10 μM control peptide or disruptor peptide for 4 h (C, D). Spontaneous tethering (rolling, transient tether, firm tether, spreading, locomotion) and detachment of the $CD4^+Foxp3^-GFP^-$ Teff cells (A, C) and $CD4^+Foxp3^+GFP^+$ Treg cells (B,D) while interacting with high density ICAM-1-Fc (5 μg/ml) were analyzed under flow. Data represent mean ± SEM results from 3 independent experiments and are expressed as percentage of total cells that accumulate in the flow chamber before the flow starts. Percentage of cells in each category is normalized to the vehicle condition set at 100 percent.

Fig. S2: Firm adhesiveness of $CD4^+$ T cells to VCAM-1 is not affected by PDE8 inhibition at the catalytic moiety or by disruption of the PDE8A-Raf-1 complex.
MOG_{35-55} primed $CD4^+$ T cells isolated from the draining PLNs on day 10 post-immunization were treated with either vehicle or 1 μM PF-04957325 for 1 h (A) or 10 μM control peptide or disruptor peptide for 4 h (B). Spontaneous tethering (rolling, transient tether, firm tether, adherent cells) and detachment of the $CD4^+$ T cells while interacting with high density VCAM-1- Fc (2 μg/ml) were analyzed under shear stress of 5 dyn/cm^2. Data represent mean ± SEM results from 4 independent experiments and are expressed as percentage of total cells that accumulate in the flow chamber before the flow starts. Percentage of cells in each category is normalized to the vehicle condition set at 100 percent.

Fig. S3: Integrin surface expression is not altered by PDE8 inhibition at the catalytic moiety and marginally reduced by disruption of the PDE8A-Raf-1 complex.
$CD4^+$ T cells isolated from spleens of *Foxp3gfp.KI* mice were treated with plate-bound anti-CD3 (10 μg/ml) for 18 h followed by treatment with vehicle or 1 μM PF-04957325 for 1 h or 10 μM control peptide or PDE8A-Raf-1 disruptor peptide for 4 h. Expression of αL integrin, α4 integrin, and CD44 was evaluated by flow cytometry. Data show MFI of the αL^+, $\alpha 4^+$ and $CD44^+$ cells within the $Foxp3^-GFP^-$ Teff cell (A) and $Foxp3^+GFP^+$ Treg cell populations (B). Data represent mean ± SEM results from 1 experiment (n=3).

Fig. S4: Inhibition of PDE8 or disruption of the PDE8A-Raf-1 complex does not affect viability of $CD4^+$ T cells.
$CD4^+$ T cells isolated from spleens of *Foxp3gfp.KI* mice were treated with plate-bound anti-CD3 (10 μg/ml) for 18 h followed by treatment with vehicle or 1 μM PF-04957325 for 1 h or 10 μM control peptide or PDE8A-Raf-1 disruptor peptide for 4 h.

The viability of the $CD4^+$ T cells after treatment was assessed using the trypan blue assay. The graphs represent the percentage of live and dead cells within each treatment group. Data represent mean ± SEM results from 1 experiment (n=3).

Supplemental Movies:

Movie S1: Naive Teff cells isolated from spleens of wild type C57BL/6 mice interacting with LPS activated brain endothelial cells under 5 dyn/cm^2 shear stress. 152 Teff cells counted during the accumulation phase before the shear flow starts. Scale bar 100 μm.

Movie S2: Naive Treg cells isolated from spleens of wild type C57BL/6 mice interacting with LPS activated brain endothelial cells under 5 dyn/cm^2 shear stress. 130 Treg cells counted during the accumulation phase before the shear flow starts. Scale bar 100 μm.

Movie S3: Teff cells activated with anti-CD3 for 18 h followed by interaction with LPS activated brain endothelial cells under 5 dyn/cm^2 shear stress. 48 Teff cells counted during the accumulation phase before shear flow starts. Scale bar 100 μm.

Movie S4: Treg cells activated with anti-CD3 for 18 h followed by interaction with LPS activated brain endothelial cells under 5 dyn/cm^2 shear stress. 106 Treg cells counted during the accumulation phase before shear flow starts. Scale bar 100 μm.

Movie S5: Teff cells activated with anti-CD3+IL-2 for 18 h followed by interaction with LPS activated brain endothelial cells under 5 dyn/cm^2 shear stress. 120 Teff cells counted during the accumulation phase before the shear flow starts. Scale bar 100 μm.

Movie S6: Treg cells activated with anti-CD3+IL-2 for 18 h followed by interaction with LPS activated brain endothelial cells under 5 dyn/cm^2 shear stress. 39 Treg cells counted during the accumulation phase before the shear flow starts. Scale bar 100 μm.

Movie S7: MOG_{35-55} activated $CD4^+$ T cells isolated from draining lymph nodes of *Foxp3gfp.KI* mice and LPS activated brain endothelial cells were treated with vehicle control for 45 min followed by interaction with LPS activated brain endothelial cells under 5 dyn/cm^2 shear stress. 140 $Foxp3^-GFP^-$ Teff cells and 27 $Foxp3^+GFP^+$ Treg cells counted during the accumulation phase before flow starts. Scale bar 100 μm.

Movie S8: MOG_{35-55} activated $CD4^+$ T cells isolated from draining lymph nodes of *Foxp3gfp.KI* mice and LPS activated brain endothelial cells were treated with PF-04957325 for 45 min followed by interaction with LPS activated brain endothelial cells under 5 dyn/cm^2 shear stress. 124 $Foxp3^-GFP^-$ Teff cells and 16 $Foxp3^+GFP^+$ Treg cells counted during the accumulation phase before flow starts. Scale bar 100 μm.

Movie S9: MOG_{35-55} activated $CD4^+$ T cells isolated from draining lymph nodes of *Foxp3gfp.KI* mice and LPS activated brain endothelial cells were treated with control peptide for 4 h followed by interaction with LPS activated brain endothelial cells under 5 dyn/cm^2 shear stress. 333 $Foxp3^-GFP^-$ Teff cells and 22 $Foxp3^+GFP^+$ Treg cells counted during the accumulation phase before flow starts. Scale bar 100 μm.

Movie S10: MOG_{35-55} activated $CD4^+$ T cells isolated from draining lymph nodes of *Foxp3gfp.KI* mice and LPS activated brain endothelial cells were treated with disruptor peptide for 4 h followed by interaction with LPS activated brain endothelial cells under 5 dyn/cm^2 shear stress. 233 $Foxp3^-GFP^-$ Teff cells and 20 $Foxp3^+GFP^+$ Treg cells counted during the accumulation phase before flow starts. Scale bar 100 μm.

Movie S11: MOG_{35-55} activated $CD4^+$ T cells isolated from draining lymph nodes of *Foxp3gfp.KI* mice were treated with control peptide for 4 h followed by interaction with recombinant ICAM-1-Fc coated plates under 5 dyn/cm^2 shear flow. 396 $Foxp3^-GFP^-$ Teff cells and 23 $Foxp3^+GFP^+$ Treg cells counted during the accumulation phase before the flow starts.

Movie S12: MOG_{35-55} activated $CD4^+$ T cells isolated from draining lymph nodes of *Foxp3gfp.KI* mice were treated with disruptor peptide for 4 h followed by interaction with recombinant ICAM-1-Fc coated plates under 5 dyn/cm^2 shear flow. 304 $Foxp3^-GFP^-$ Teff cells and 14 $Foxp3^+GFP^+$ Treg cells counted during the accumulation phase before the flow starts.

Figure S1

A

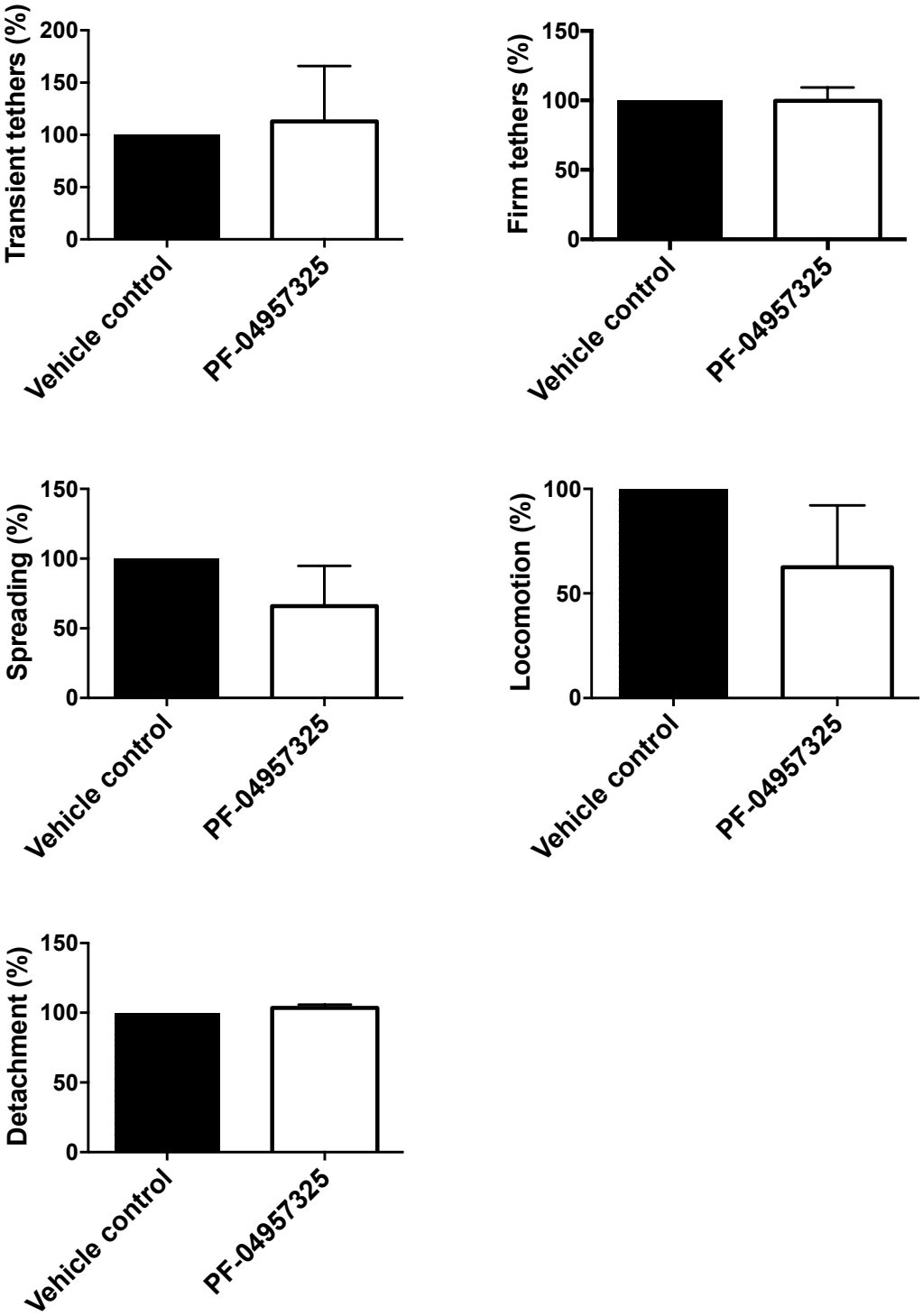
Transient tethers (%)
200
150
100
50
0
Vehicle control
PF-04957325
Firm tethers (%)
150
100
50
0
Vehicle control
PF-04957325
Spreading (%)
150
100
50
0
Vehicle control
PF-04957325
Locomotion (%)
100
50
0
Vehicle control
PF-04957325
Detachment (%)
150
100
50
0
Vehicle control
PF-04957325

Figure S1

B

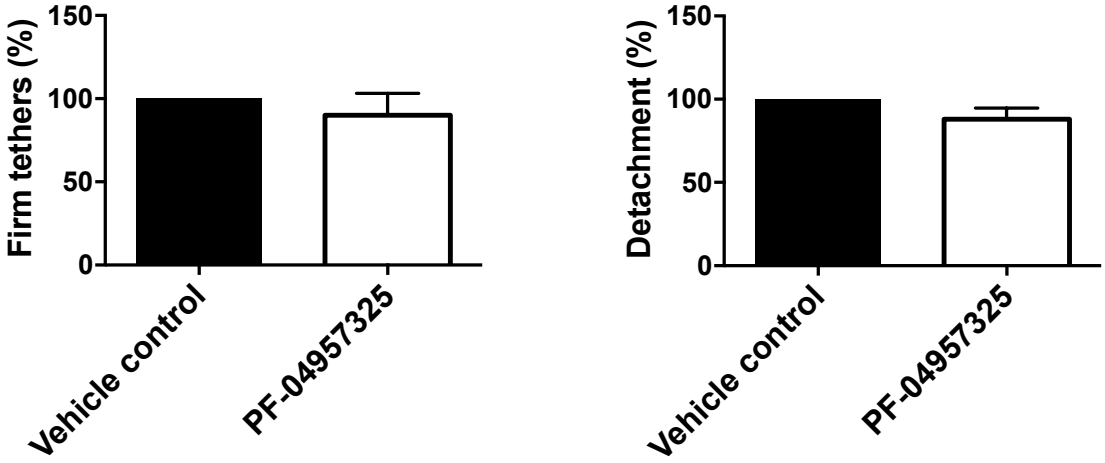
Firm tethers (%)
150
100
50
0
Vehicle control
PF-04957325
Detachment (%)
150
100
50
0
Vehicle control
PF-04957325

Figure S1

C

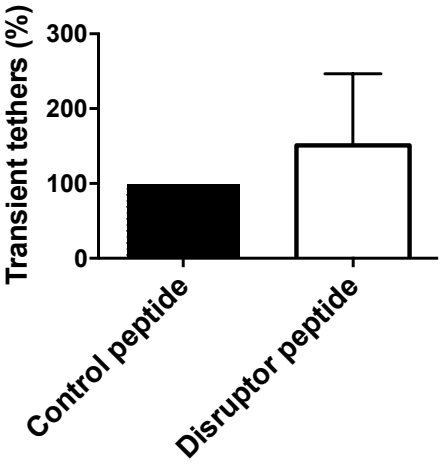
Transient tethers (%)
300
200
100
0
Control peptide
Disruptor peptide

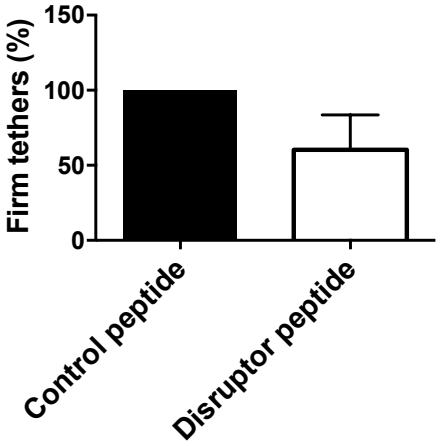
Firm tethers (%)
150
100
50
0
Control peptide
Disruptor peptide

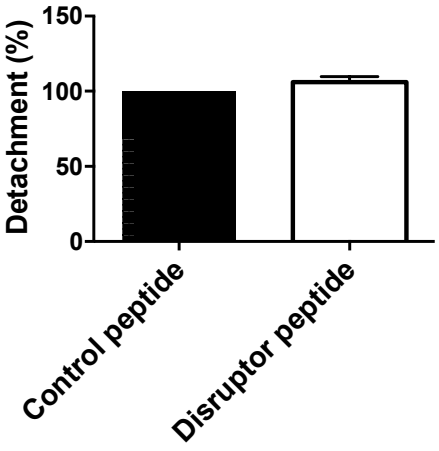
Detachment (%)
150
100
50
0
Control peptide
Disruptor peptide

D

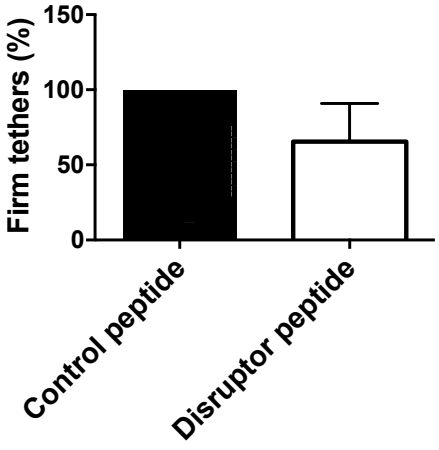
Firm tethers (%)
150
100
50
0
Control peptide
Disruptor peptide

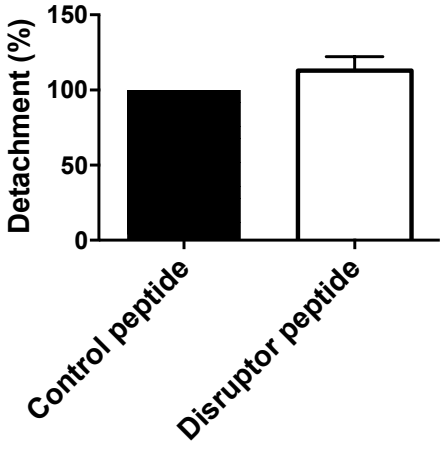
Detachment (%)
150
100
50
0
Control peptide
Disruptor peptide

Figure S2

A

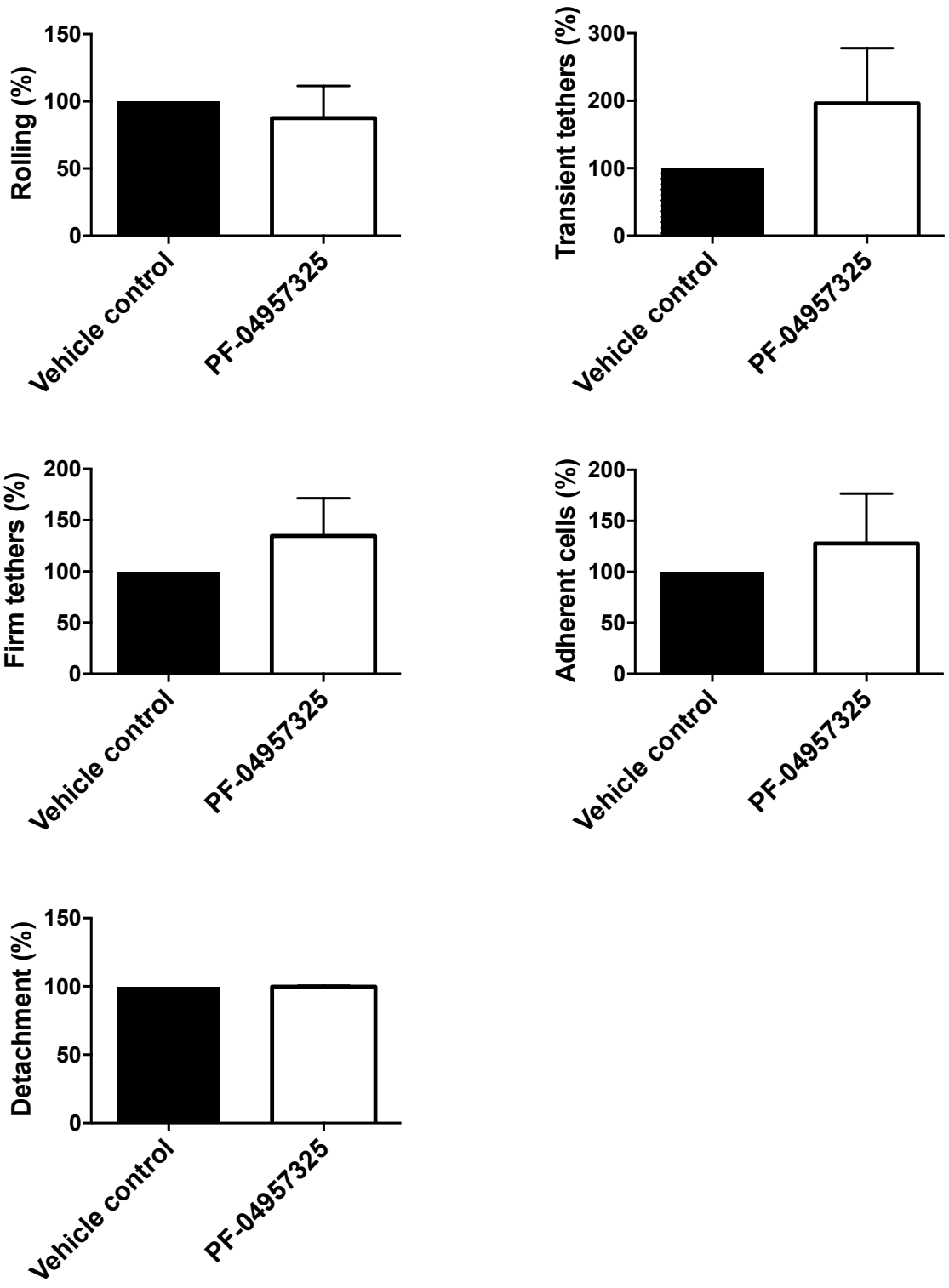
Rolling (%)
150
100
50
0
Vehicle control
PF-04957325
Transient tethers (%)
300
200
100
0
Vehicle control
PF-04957325
Firm tethers (%)
200
150
100
50
0
Vehicle control
PF-04957325
Adherent cells (%)
200
150
100
50
0
Vehicle control
PF-04957325
Detachment (%)
150
100
50
0
Vehicle control
PF-04957325

Figure S2

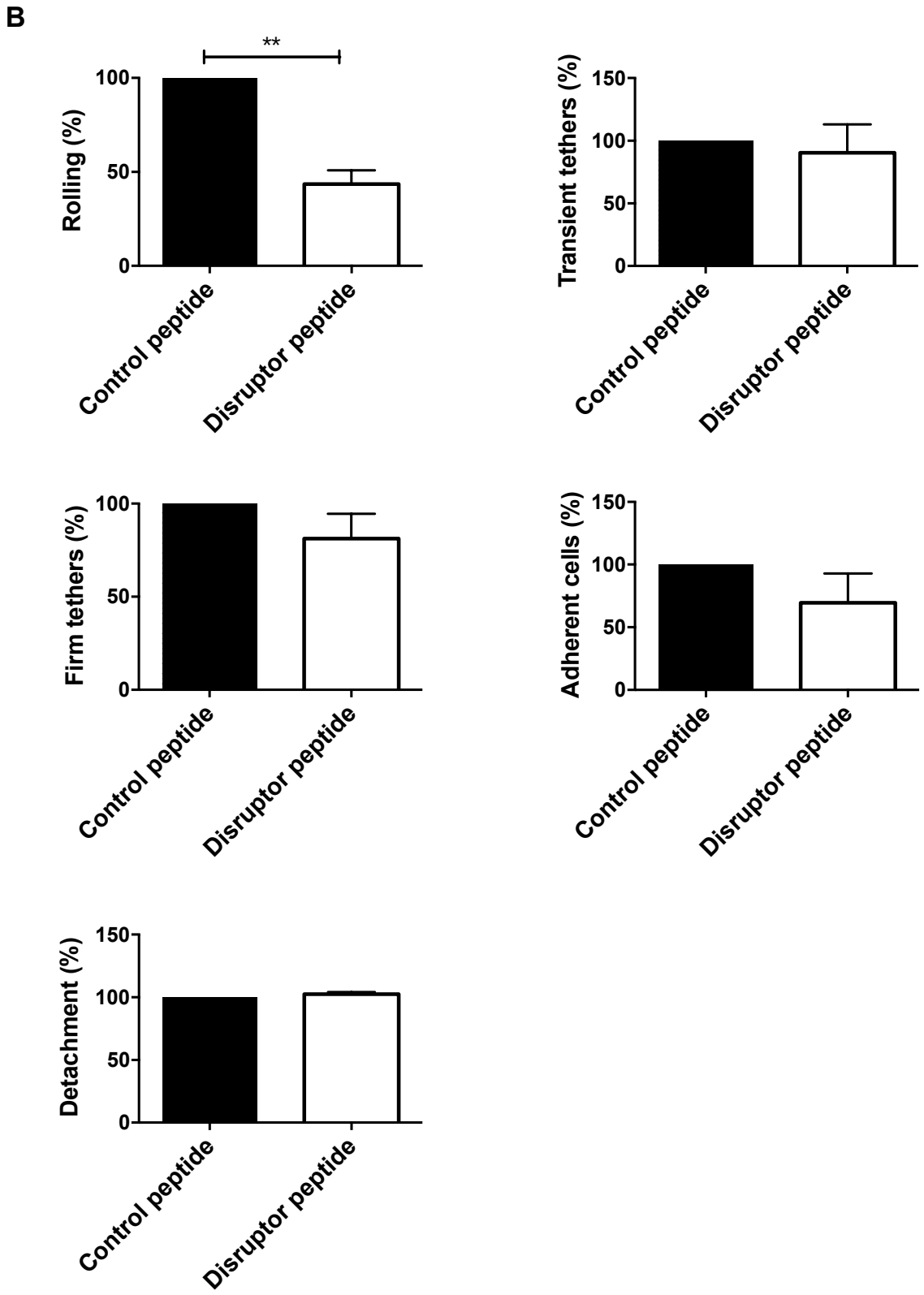
B
**
Rolling (%)
100
50
0
Control peptide
Disruptor peptide
Transient tethers (%)
150
100
50
0
Control peptide
Disruptor peptide
Firm tethers (%)
100
50
0
Control peptide
Disruptor peptide
Adherent cells (%)
150
100
50
0
Control peptide
Disruptor peptide
Detachment (%)
150
100
50
0
Control peptide
Disruptor peptide

Figure S3

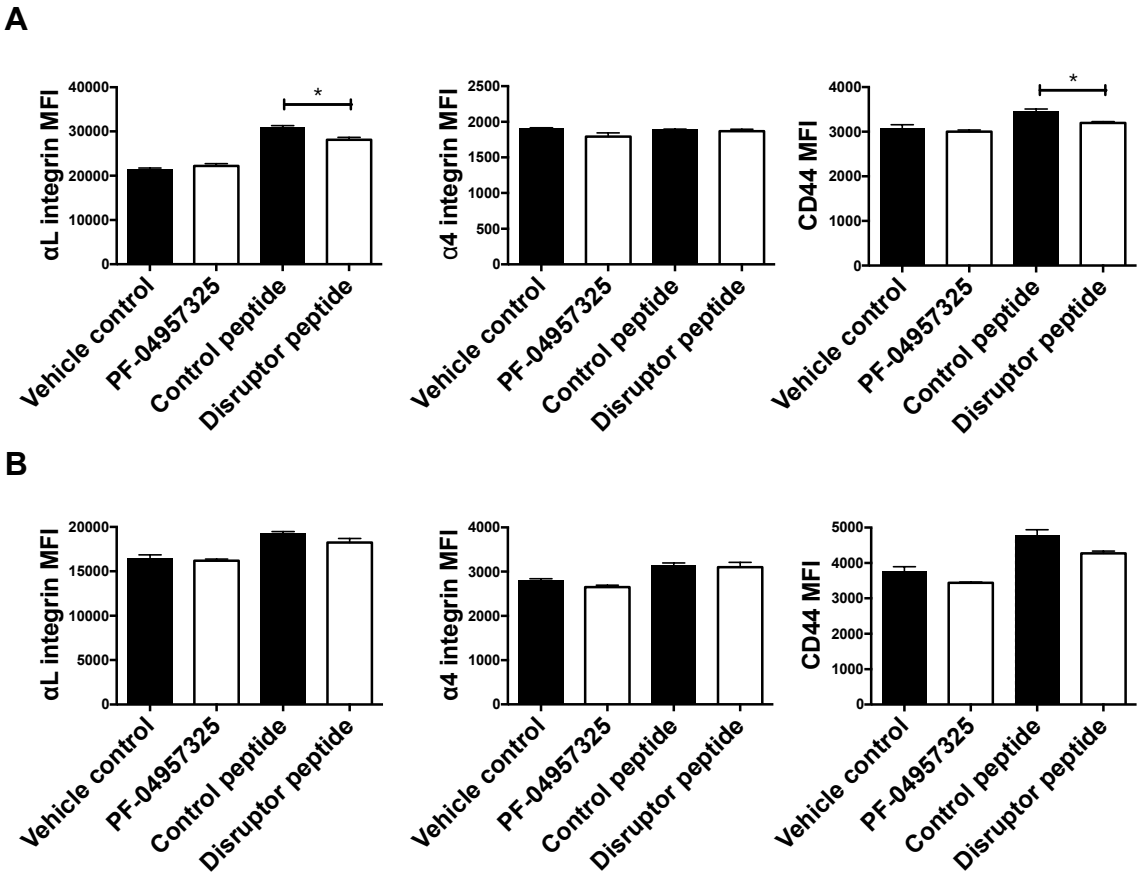
A
αL integrin MFI
40000
30000
20000
10000
0
*
α4 integrin MFI
2500
2000
1500
1000
500
0
CD44 MFI
4000
3000
2000
1000
0
*
Vehicle control
PF-04957325
Control peptide
Disruptor peptide
B
αL integrin MFI
20000
15000
10000
5000
0
α4 integrin MFI
4000
3000
2000
1000
0
CD44 MFI
5000
4000
3000
2000
1000
0
Vehicle control
PF-04957325
Control peptide
Disruptor peptide

Figure S4

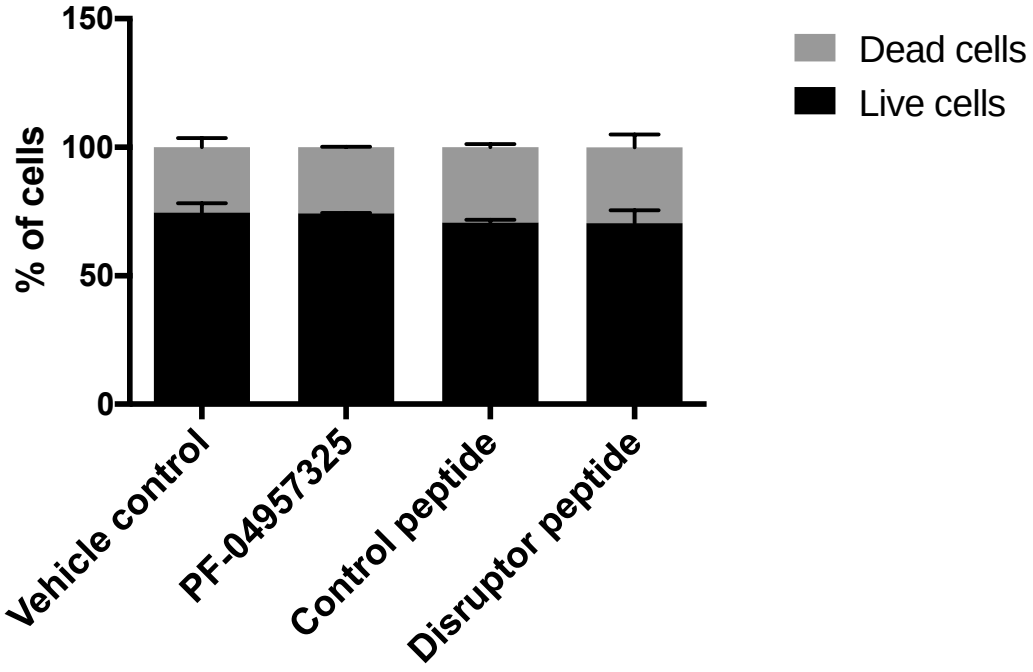
150
100
50
0
% of cells
Dead cells
Live cells
Vehicle control
PF-04957325
Control peptide
Disruptor peptide

Supplemental Movies

Still images

Movie S1

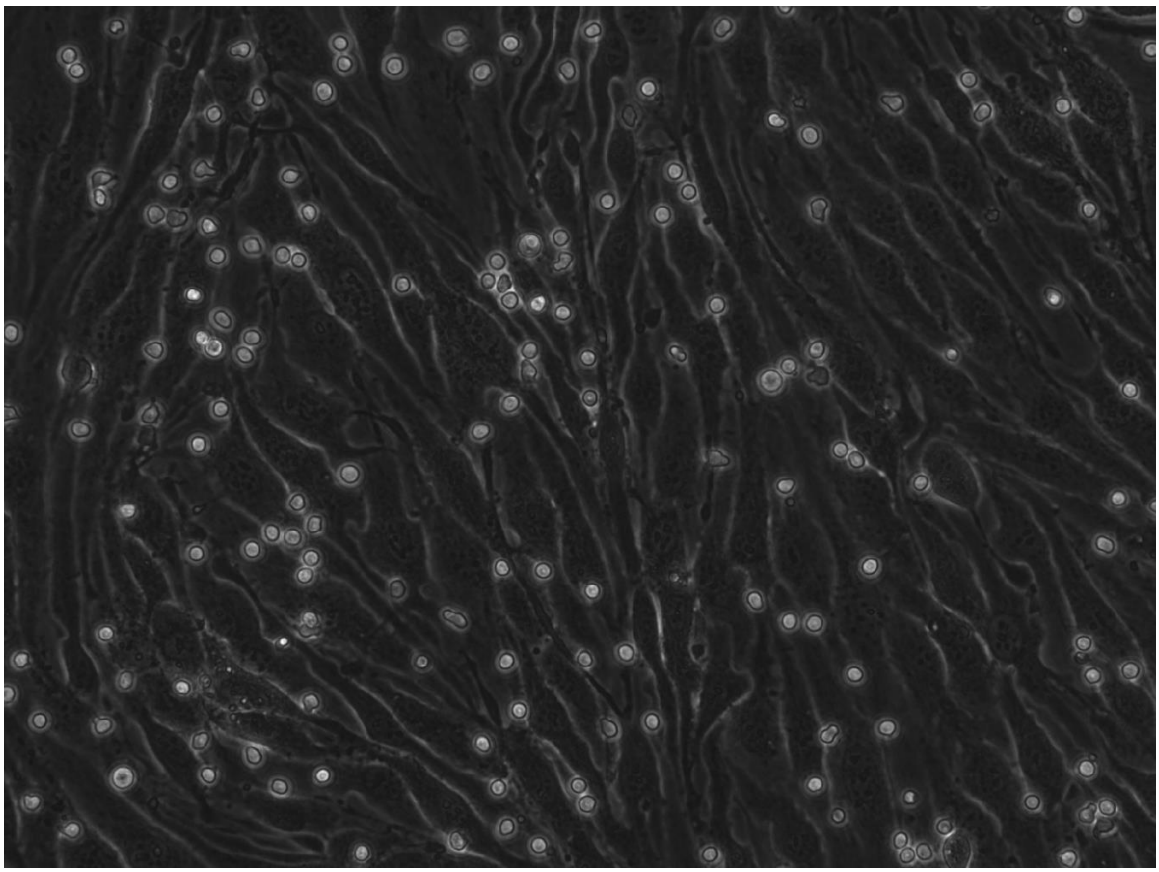

Movie S1: Naive Teff cells isolated from spleens of wild type C57BL/6 mice interacting with LPS activated brain endothelial cells under 5 dyn/cm^2 shear stress. 152 Teff cells counted during the accumulation phase before the shear flow starts.

Movie S2

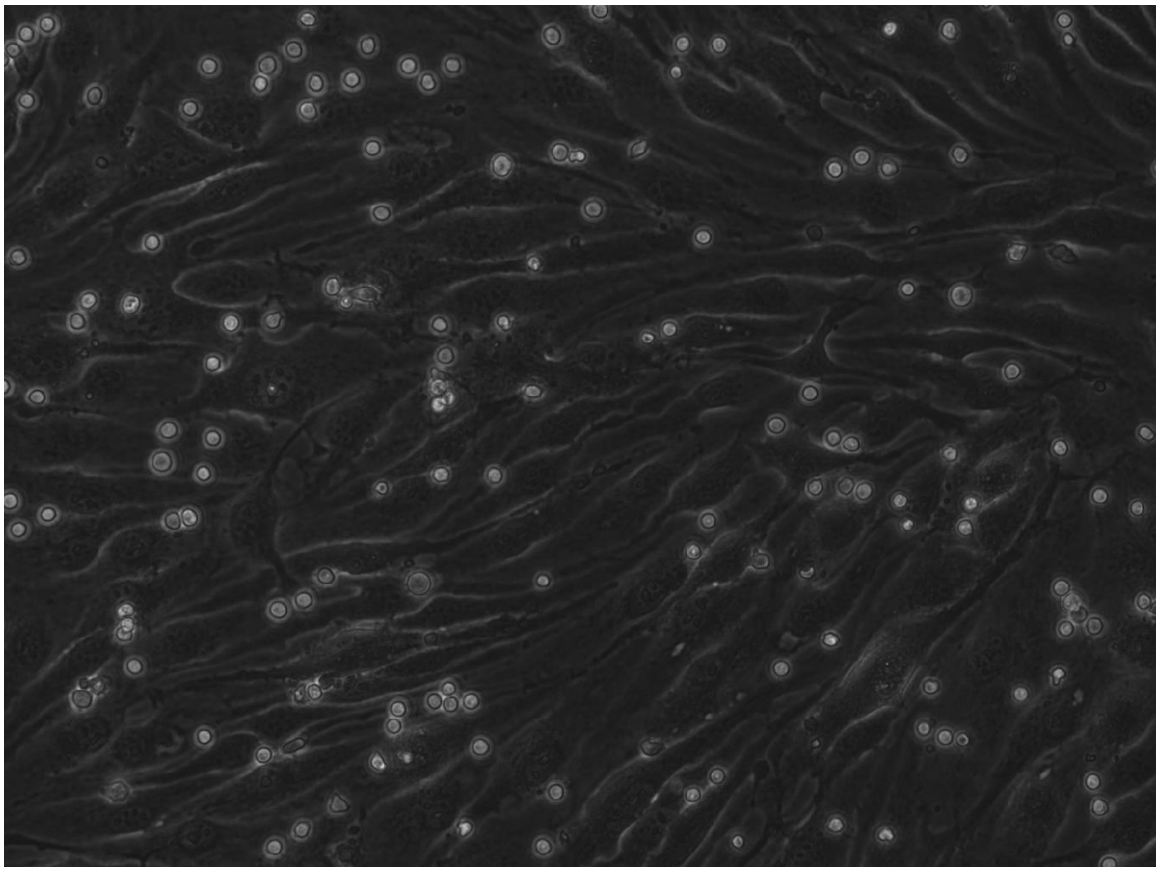

Movie S2: Naive Treg cells isolated from spleens of wild type C57BL/6 mice interacting with LPS activated brain endothelial cells under 5 dyn/cm^2 shear stress. 130 Treg cells counted during the accumulation phase before the shear flow starts.

Movie S3

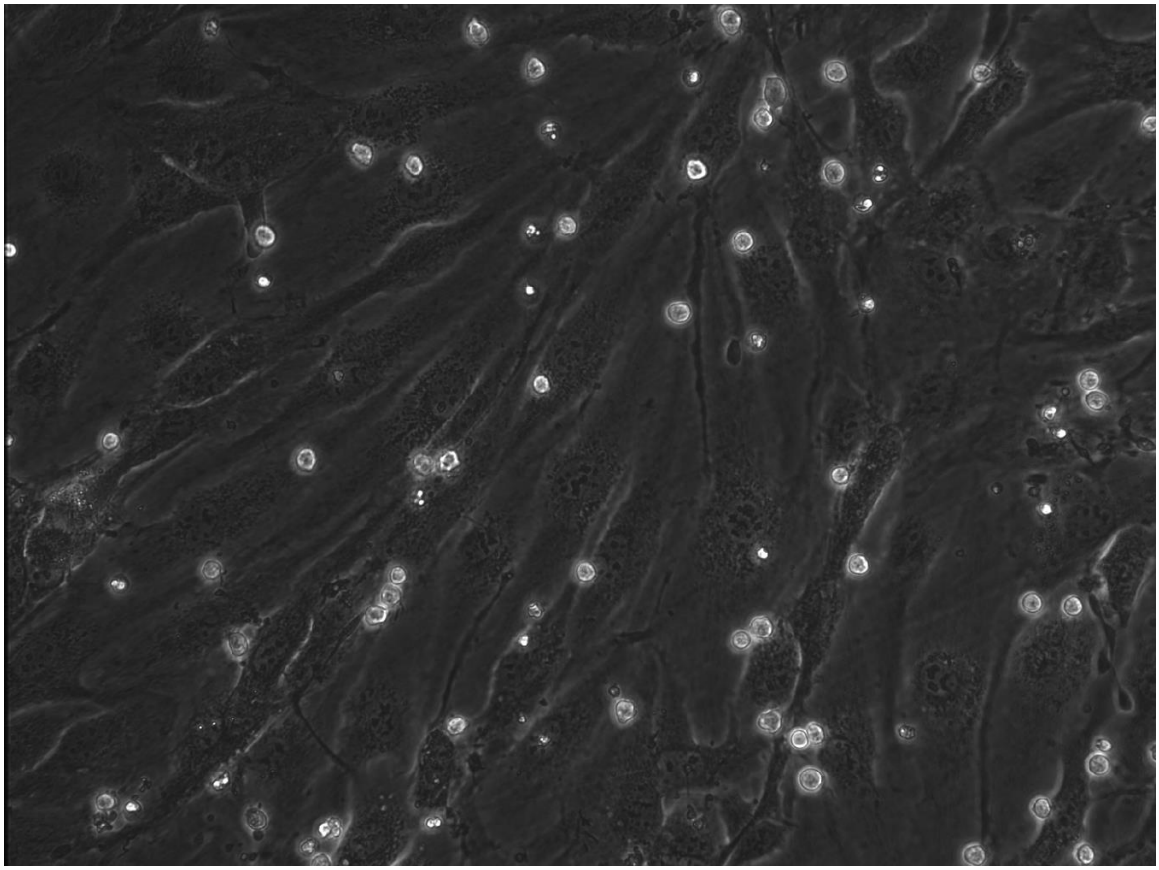

Movie S3: Teff cells activated with anti-CD3 for 18 h followed by interaction with LPS activated brain endothelial cells under 5 dyn/cm^2 shear stress. 48 Teff cells counted during the accumulation phase before shear flow starts.

Movie S4

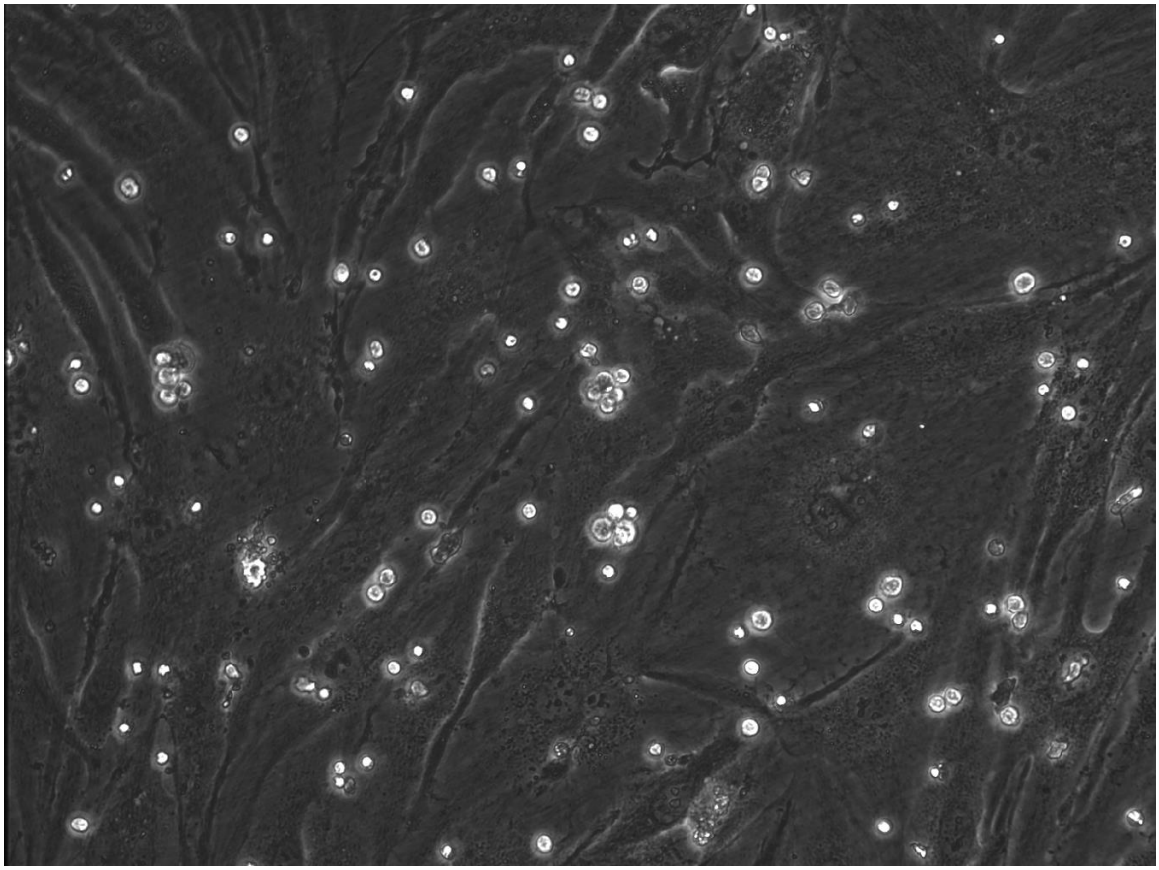

Movie S4: Treg cells activated with anti-CD3 for 18 h followed by interaction with LPS activated brain endothelial cells under 5 dyn/cm^2 shear stress. 106 Treg cells counted during the accumulation phase before shear flow starts.

Movie S5

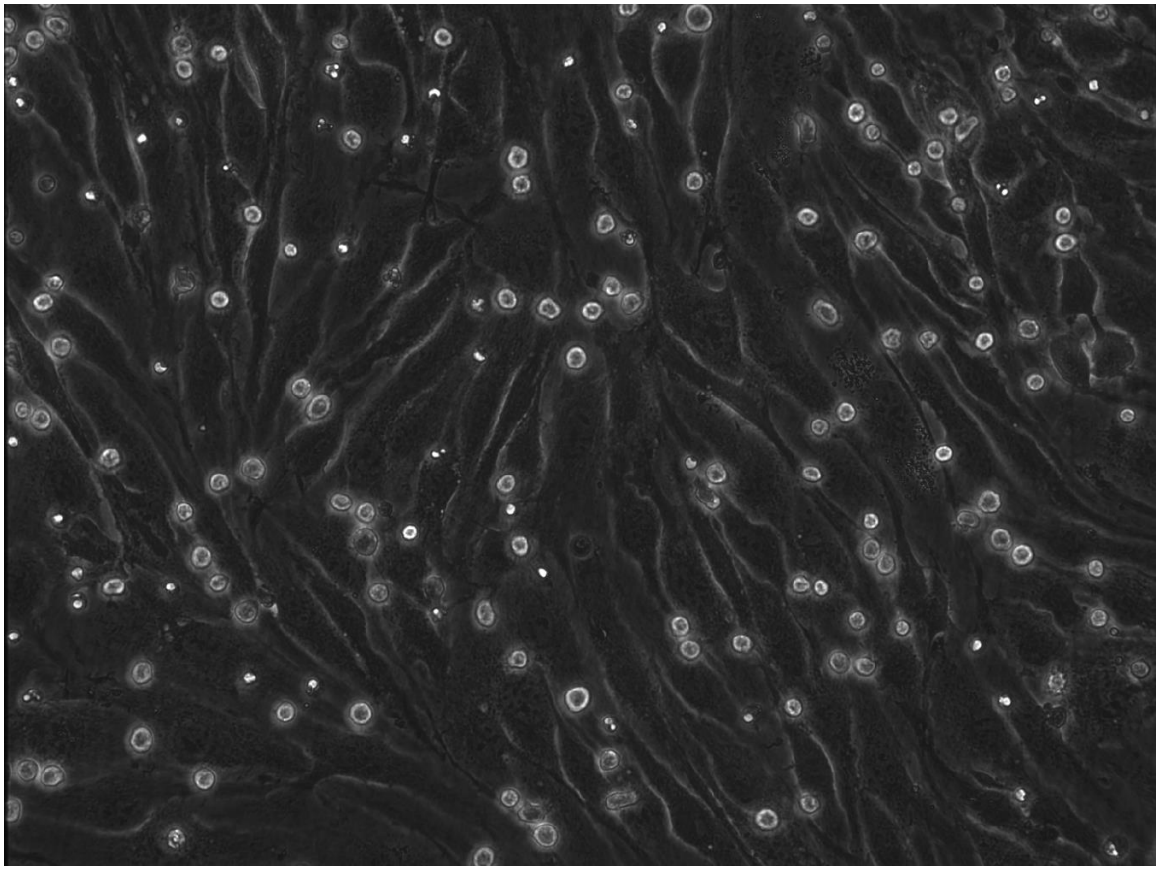

Movie S5: Teff cells activated with anti-CD3+IL-2 for 18 h followed by interaction with LPS activated brain endothelial cells under 5 dyn/cm^2 shear stress. 120 Teff cells counted during the accumulation phase before the shear flow starts.

Movie S6

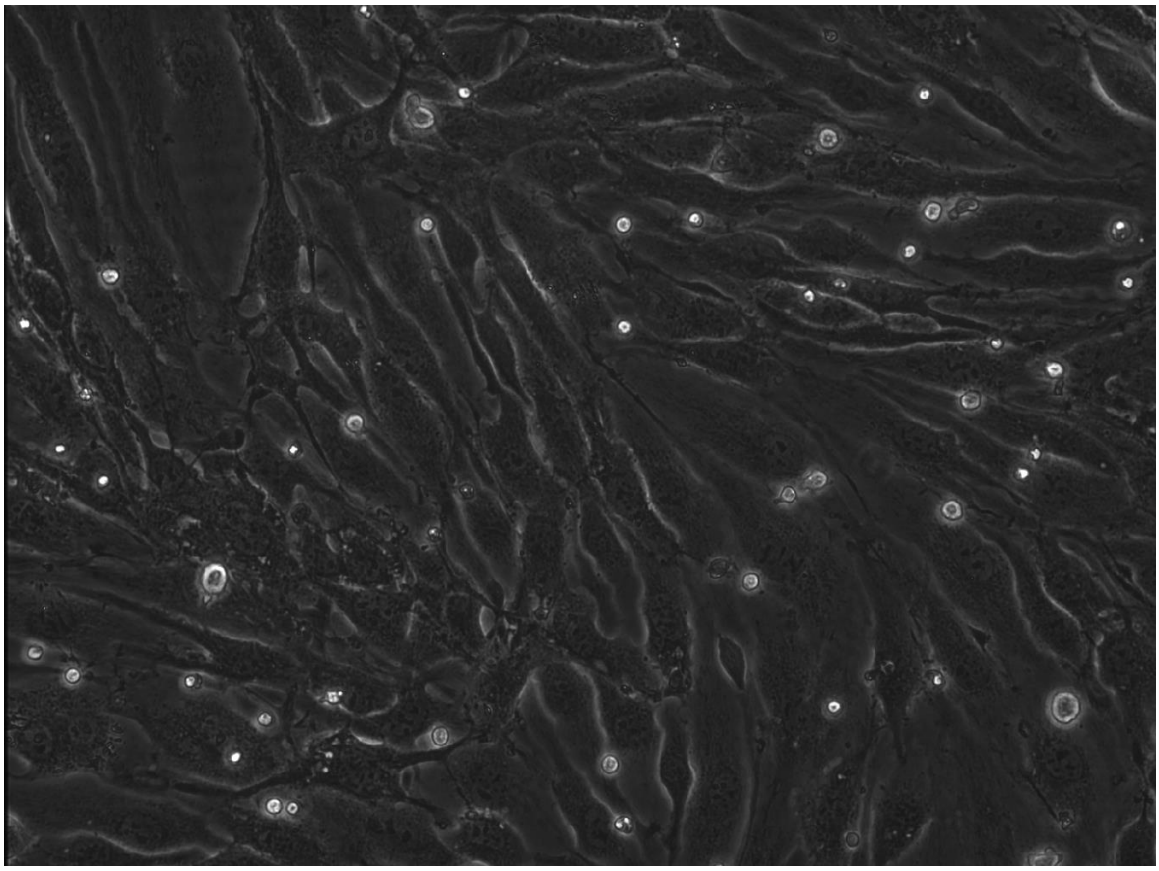

Movie S6: Treg cells activated with anti-CD3+IL-2 for 18 h followed by interaction with LPS activated brain endothelial cells under 5 dyn/cm^2 shear stress. 39 Treg cells counted during the accumulation phase before the shear flow starts.

Movie S7

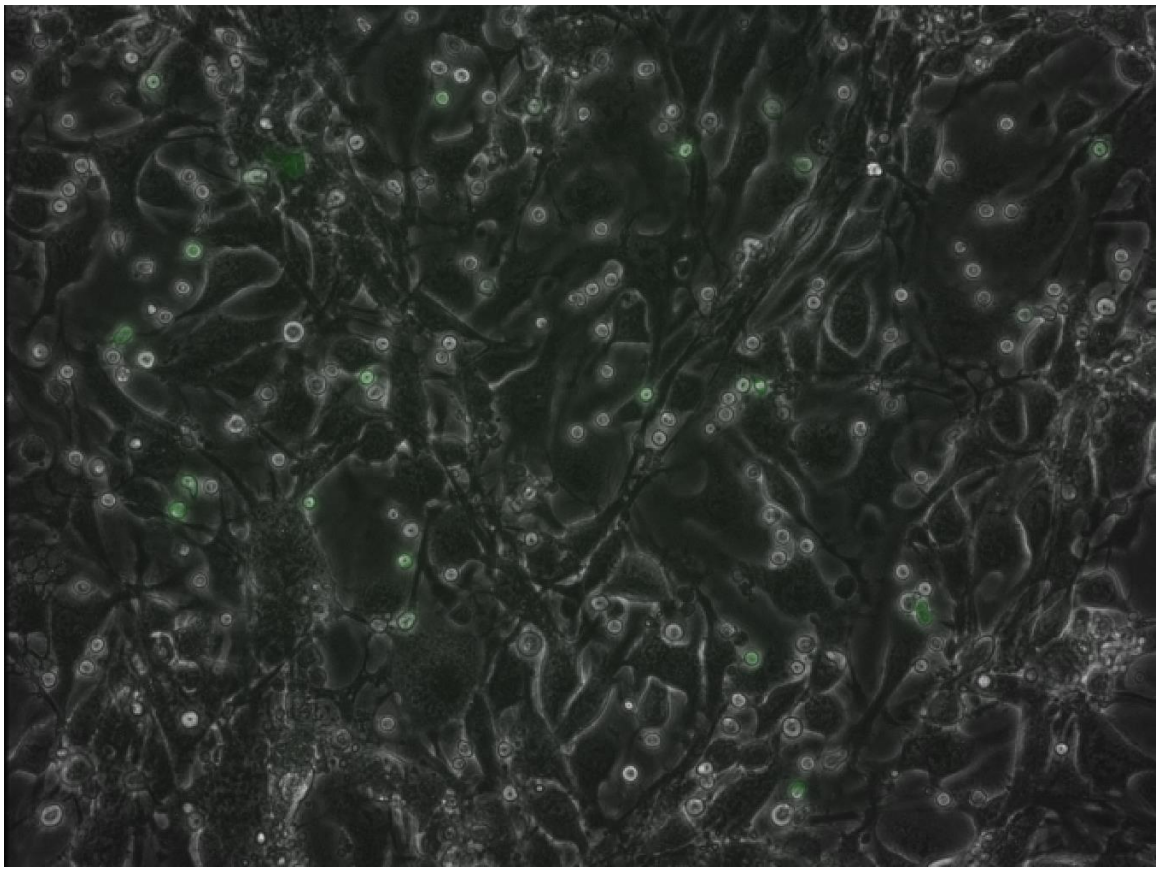

Movie S7: MOG_{35-55} activated $CD4^+$ T cells isolated from draining lymph nodes of *Foxp3gfp.KI* mice and LPS activated brain endothelial cells were treated with vehicle control for 45 min followed by interaction with LPS activated brain endothelial cells under 5 dyn/cm^2 shear stress. 140 $Foxp3^-GFP^-$ Teff cells and 27 $Foxp3^+GFP^+$ Treg cells counted during the accumulation phase before flow starts.

Movie S8

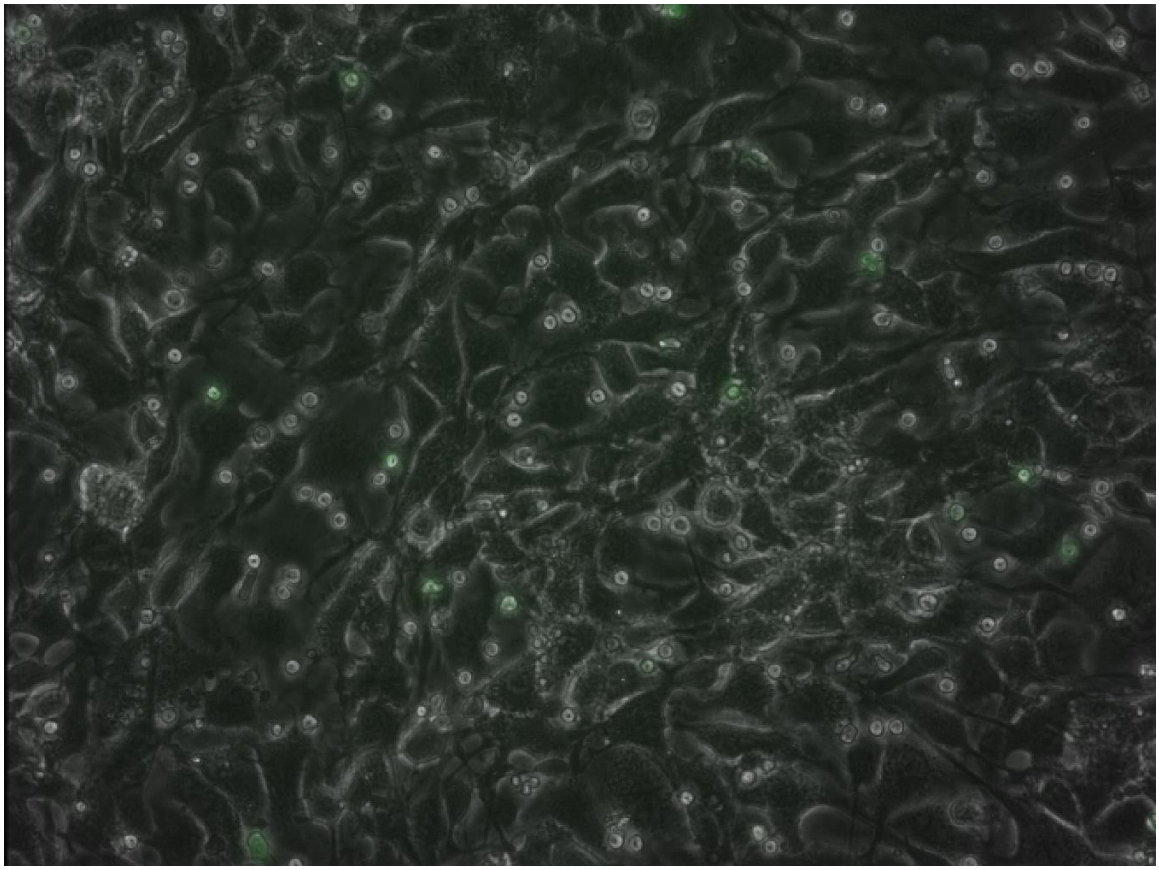

Movie S8: MOG_{35-55} activated $CD4^+$ T cells isolated from draining lymph nodes of *Foxp3gfp.KI* mice and LPS activated brain endothelial cells were treated with PF-04957325 for 45 min followed by interaction with LPS activated brain endothelial cells under 5 dyn/cm^2 shear stress. 124 $Foxp3^-GFP^-$ Teff cells and 16 $Foxp3^+GFP^+$ Treg cells counted during the accumulation phase before flow starts.

Movie S9

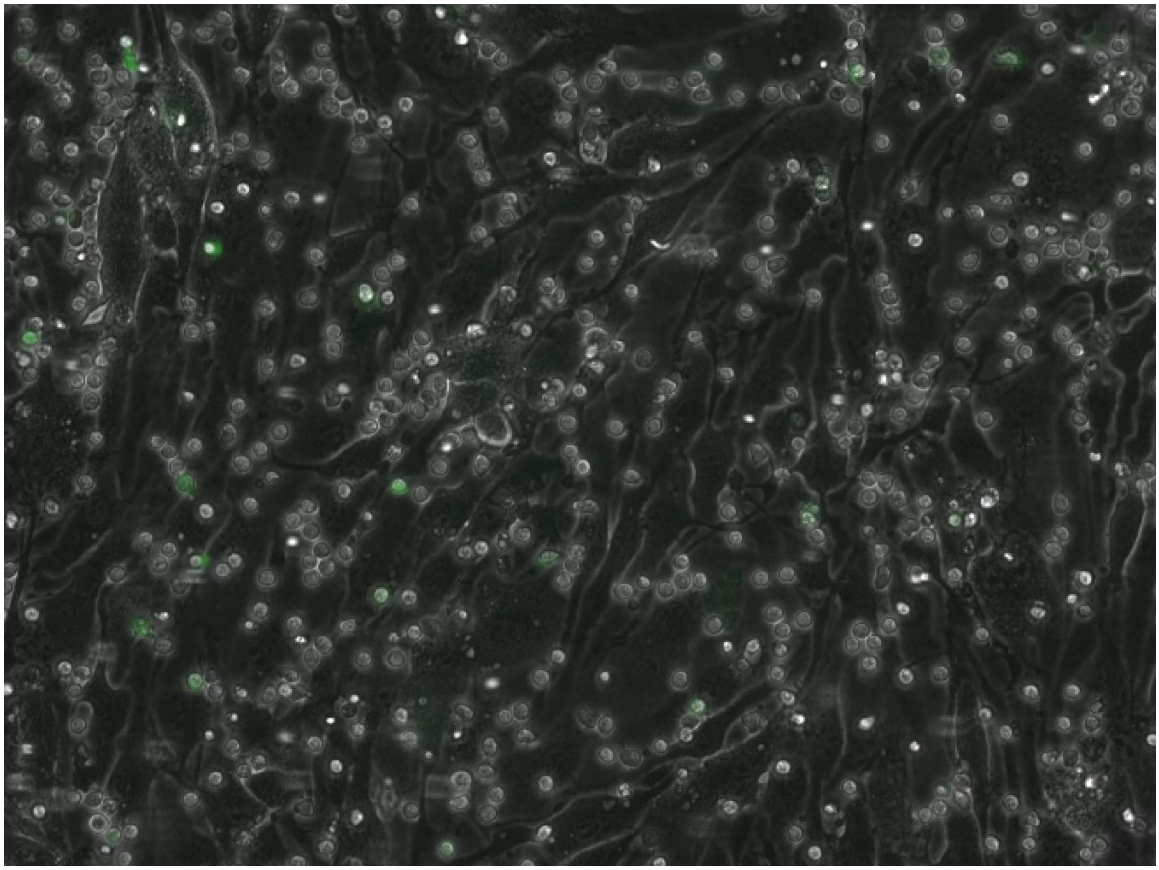

Movie S9: MOG_{35-55} activated $CD4^+$ T cells isolated from draining lymph nodes of *Foxp3gfp.KI* mice and LPS activated brain endothelial cells were treated with control peptide for 4 h followed by interaction with LPS activated brain endothelial cells under 5 dyn/cm^2 shear stress. 333 $Foxp3^-GFP^-$ Teff cells and 22 $Foxp3^+GFP^+$ Treg cells counted during the accumulation phase before flow starts.

Movie S10

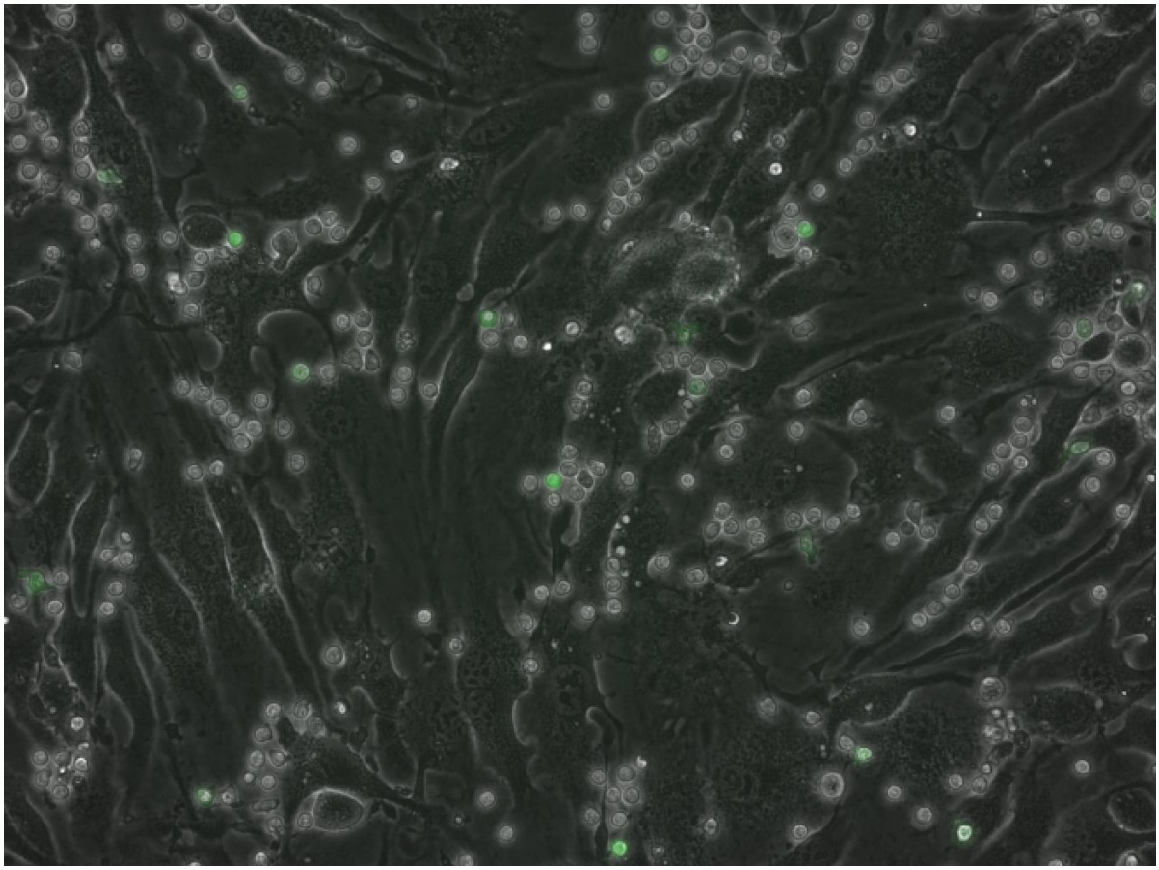

Movie S10: MOG_{35-55} activated $CD4^+$ T cells isolated from draining lymph nodes of *Foxp3gfp.KI* mice and LPS activated brain endothelial cells were treated with disruptor peptide for 4 h followed by interaction with LPS activated brain endothelial cells under 5 dyn/cm^2 shear stress. 233 $Foxp3^-GFP^-$ Teff cells and 20 $Foxp3^+GFP^+$ Treg cells counted during the accumulation phase before flow starts.

Movie S11

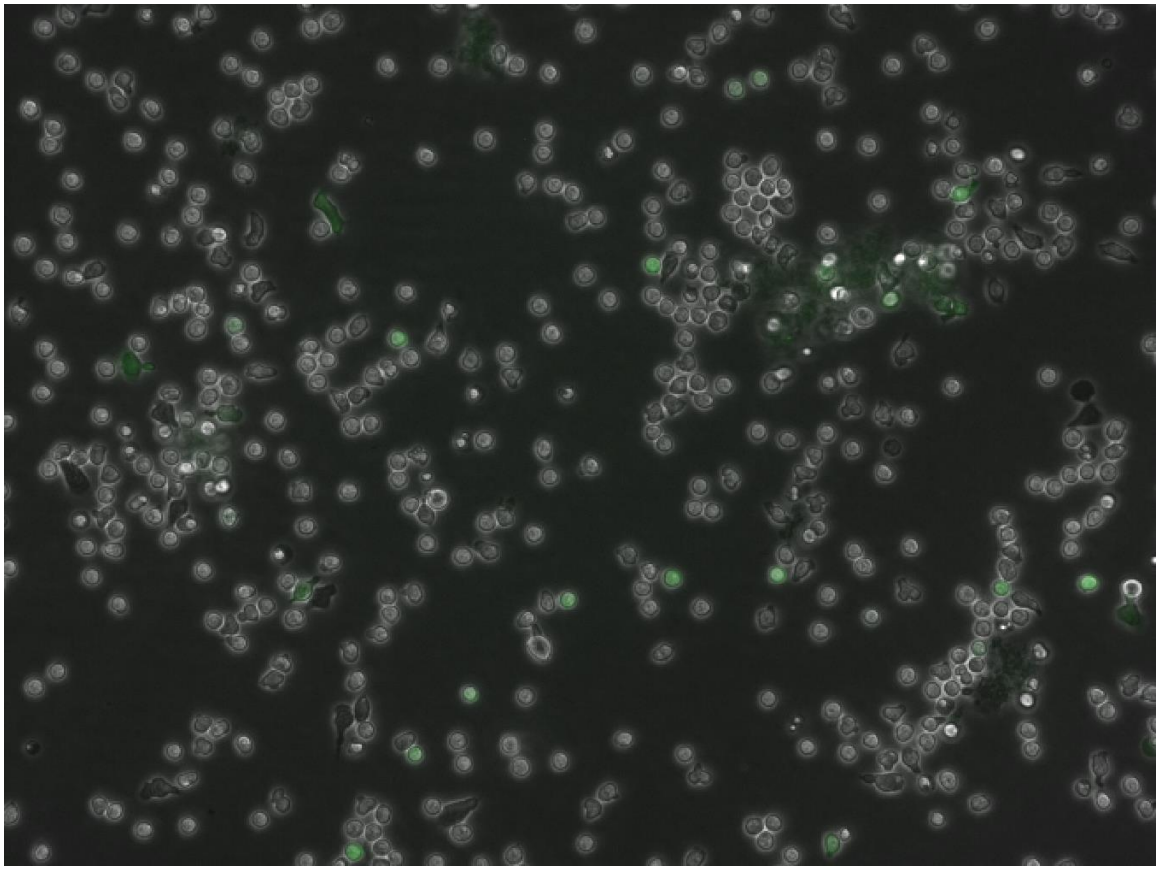

Movie S11: MOG_{35-55} activated $CD4^+$ T cells isolated from draining lymph nodes of *Foxp3gfp.KI* mice were treated with control peptide for 4 h followed by interaction with recombinant ICAM-1-Fc coated plates under 5 dyn/cm^2 shear flow. 396 $Foxp3^-GFP^-$ Teff cells and 23 $Foxp3^+GFP^+$ Treg cells counted during the accumulation phase before the flow starts.

Movie S12

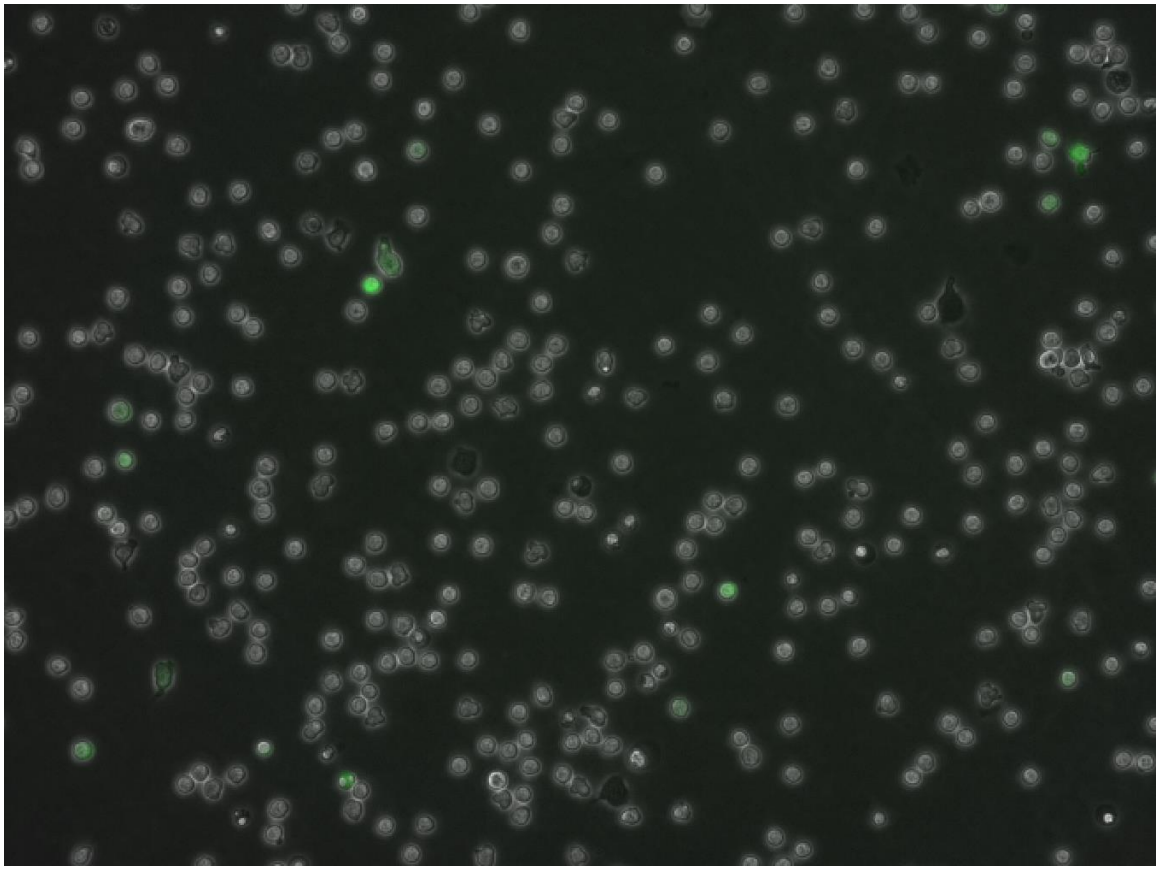

Movie S12: MOG_{35-55} activated $CD4^+$ T cells isolated from draining lymph nodes of *Foxp3gfp.KI* mice were treated with disruptor peptide for 4 h followed by interaction with recombinant ICAM-1-Fc coated plates under 5 dyn/cm^2 shear flow. 304 $Foxp3^-GFP^-$ Teff cells and 14 $Foxp3^+GFP^+$ Treg cells counted during the accumulation phase before the flow starts.